

Electrical Properties of Organic Semiconductors

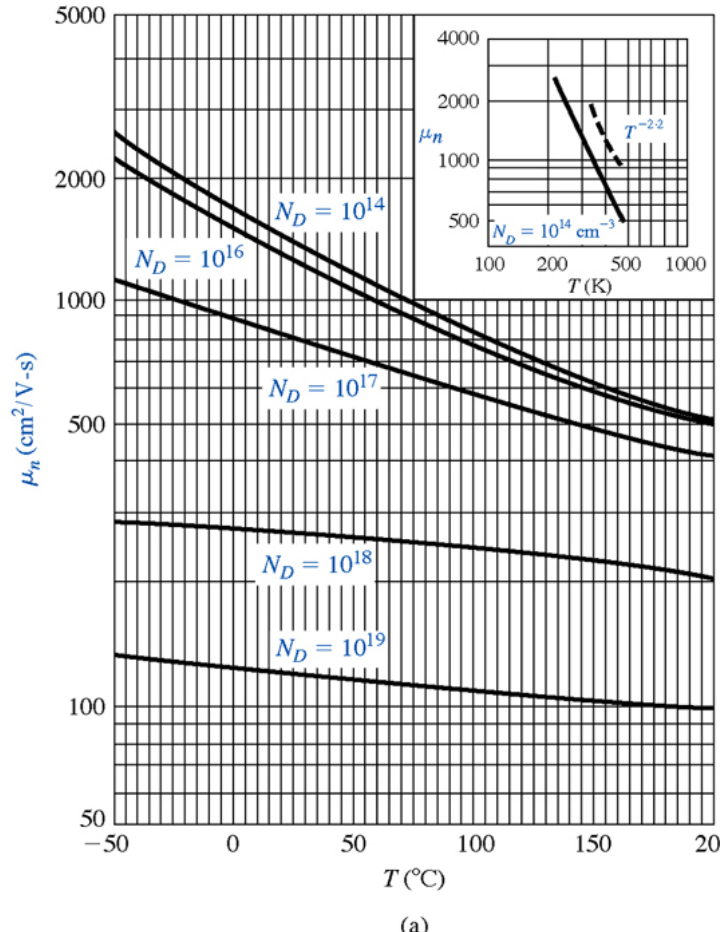
2014. 4. 17.

Changhee Lee
School of Electrical and Computer Engineering
Seoul National Univ.
chlee7@snu.ac.kr



Charge Transport in Si and Organic Crystals

Electron mobility of Si



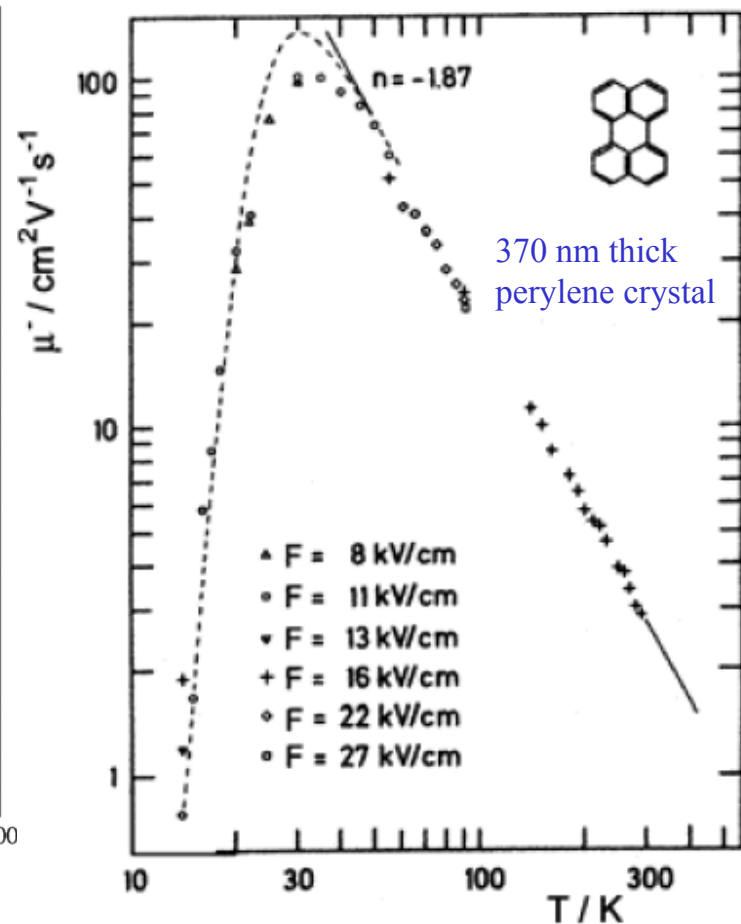
(a)

Band-like transport of carriers.

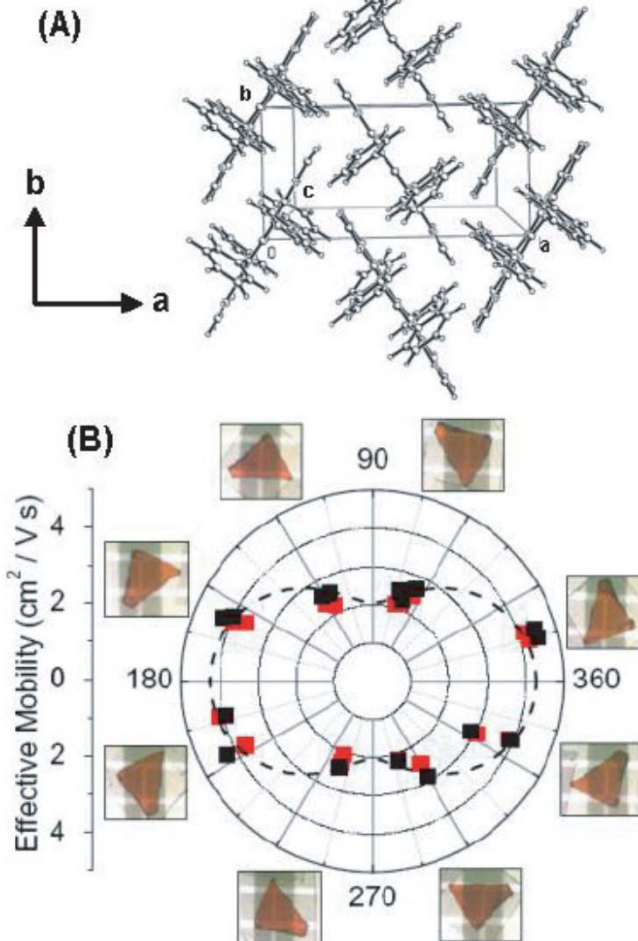
Carrier mobility is limited by scatterings with phonons, impurities, etc.

$$\mu(T) \approx \mu_0 T^{-n}$$

Electron mobility of Perylene



Rubrene crystal: The angular dependence of the mobility measured at room temperature.



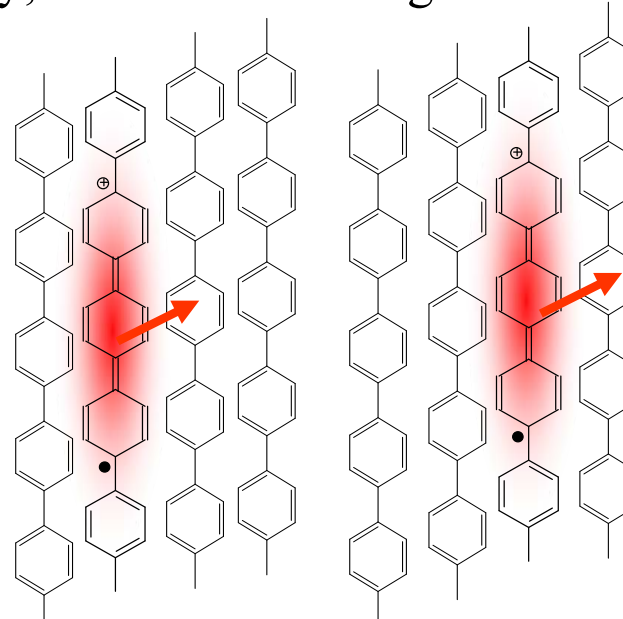
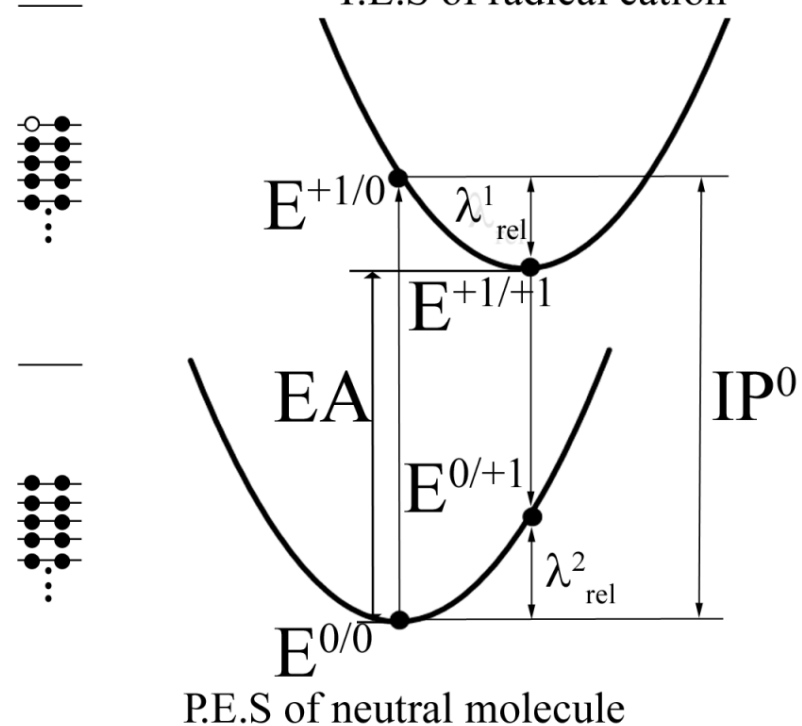
Rate of Charge Transfer

The rate of charge transfer is limited by the reorganization of the molecules.

According to the semiclassical Marcus theory in the high temperature limit, the electron - transfer (hopping) rate, k_{ET} , can be described as,

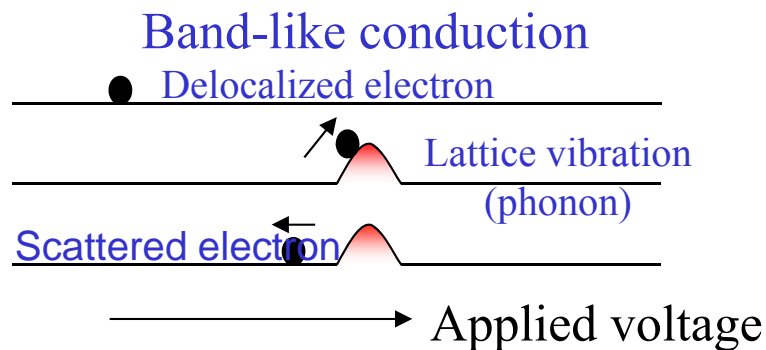
$$k_{ET} = A \cdot \exp\left[-\frac{(\lambda - 2t)^2}{4\lambda k_B T}\right]$$

T = temperature; λ = reorganization energy; t = transfer integral

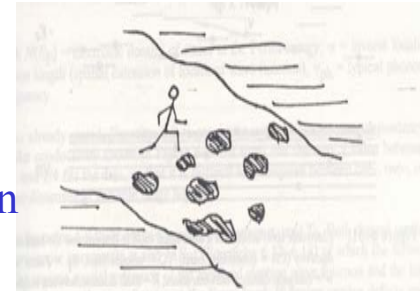
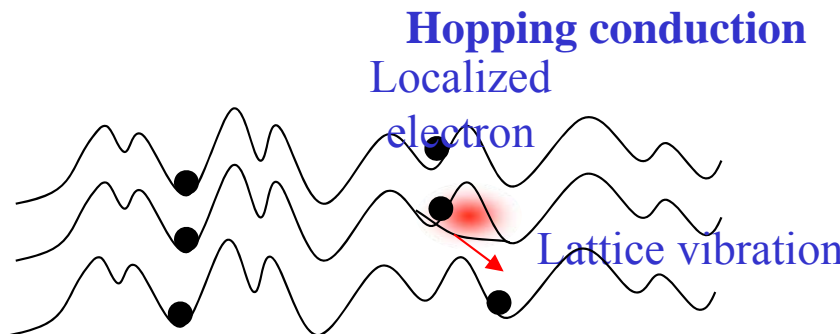
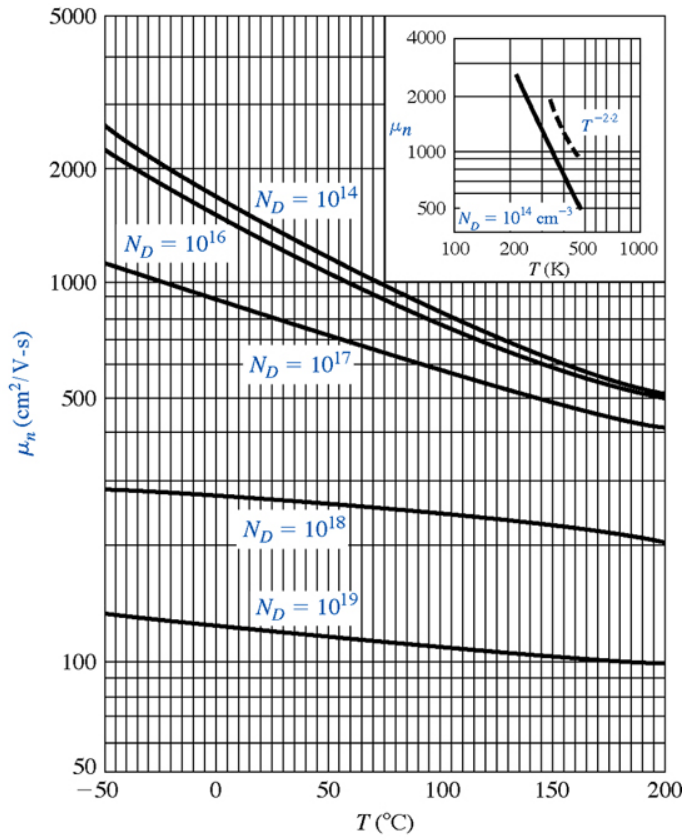


Polaron hopping

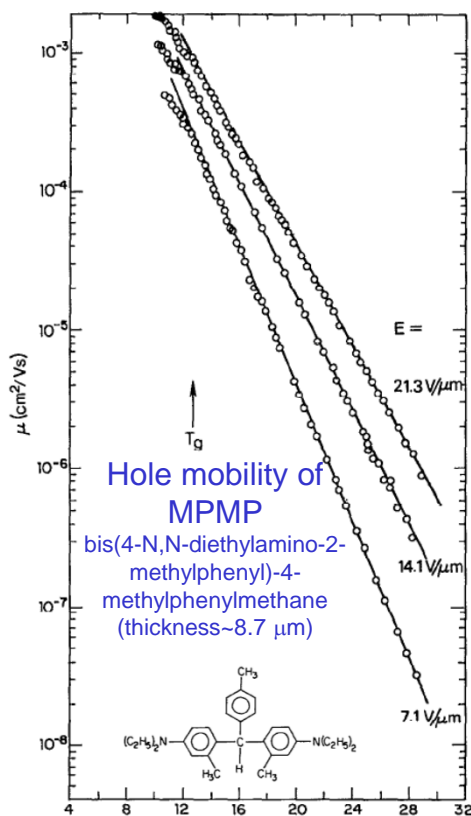
Carrier mobility



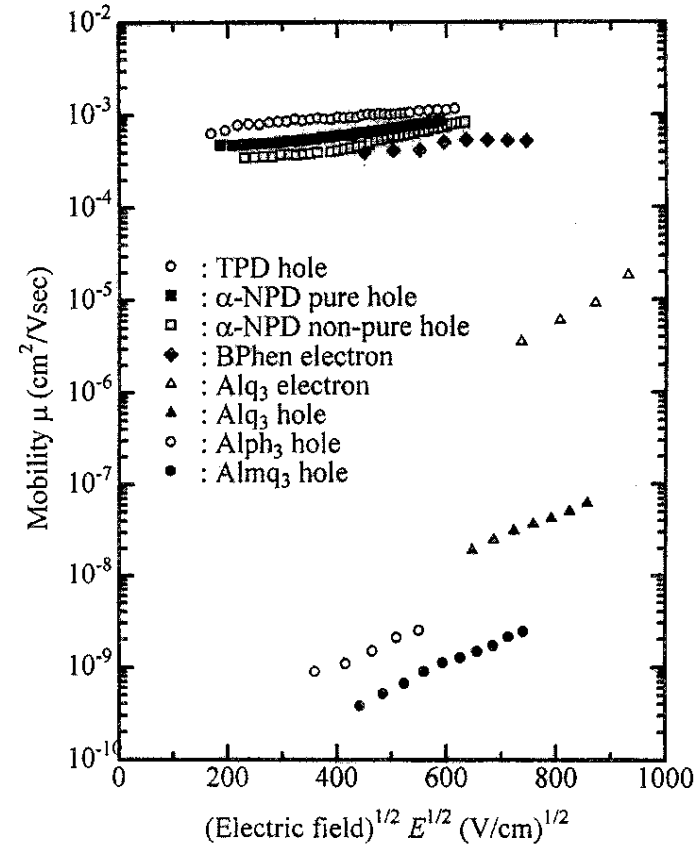
Electron mobility of Si



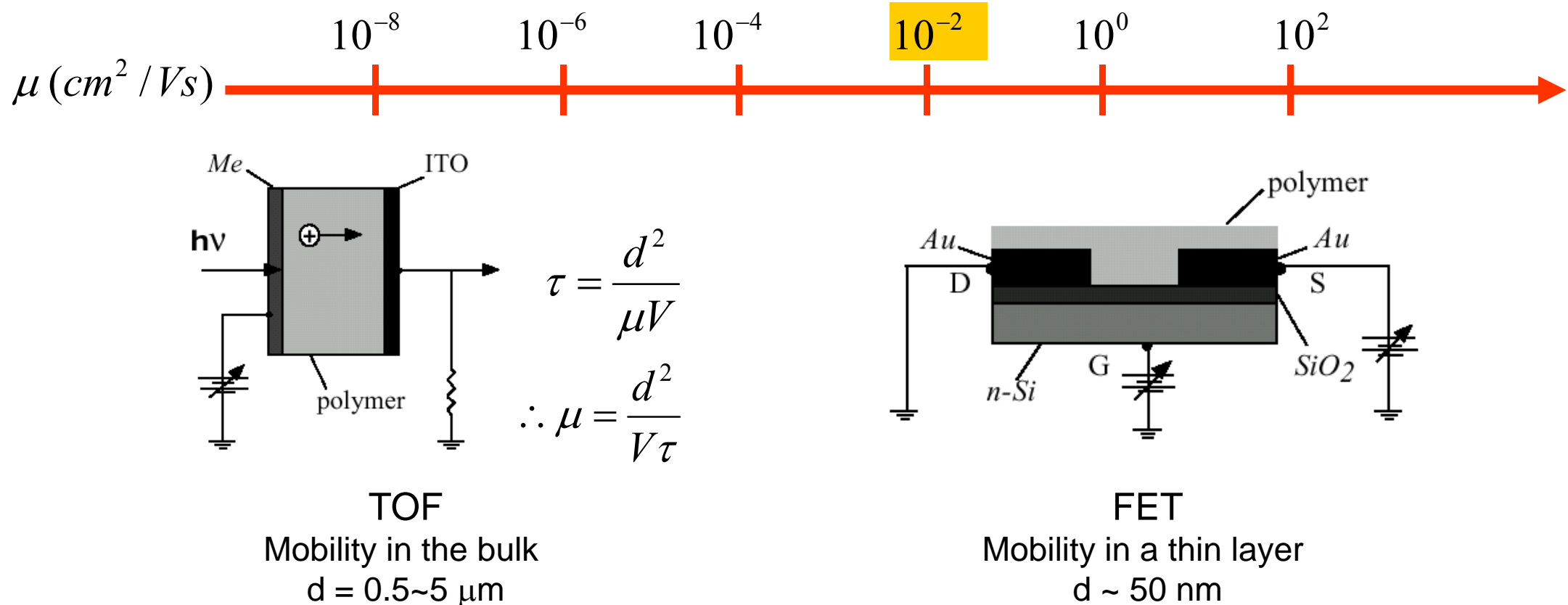
e & h mobility of organic materials



P. M. Borsenberger, L. Pautmeier and H. Bässler, J. Chem. Phys. 95, 1258 (1991)



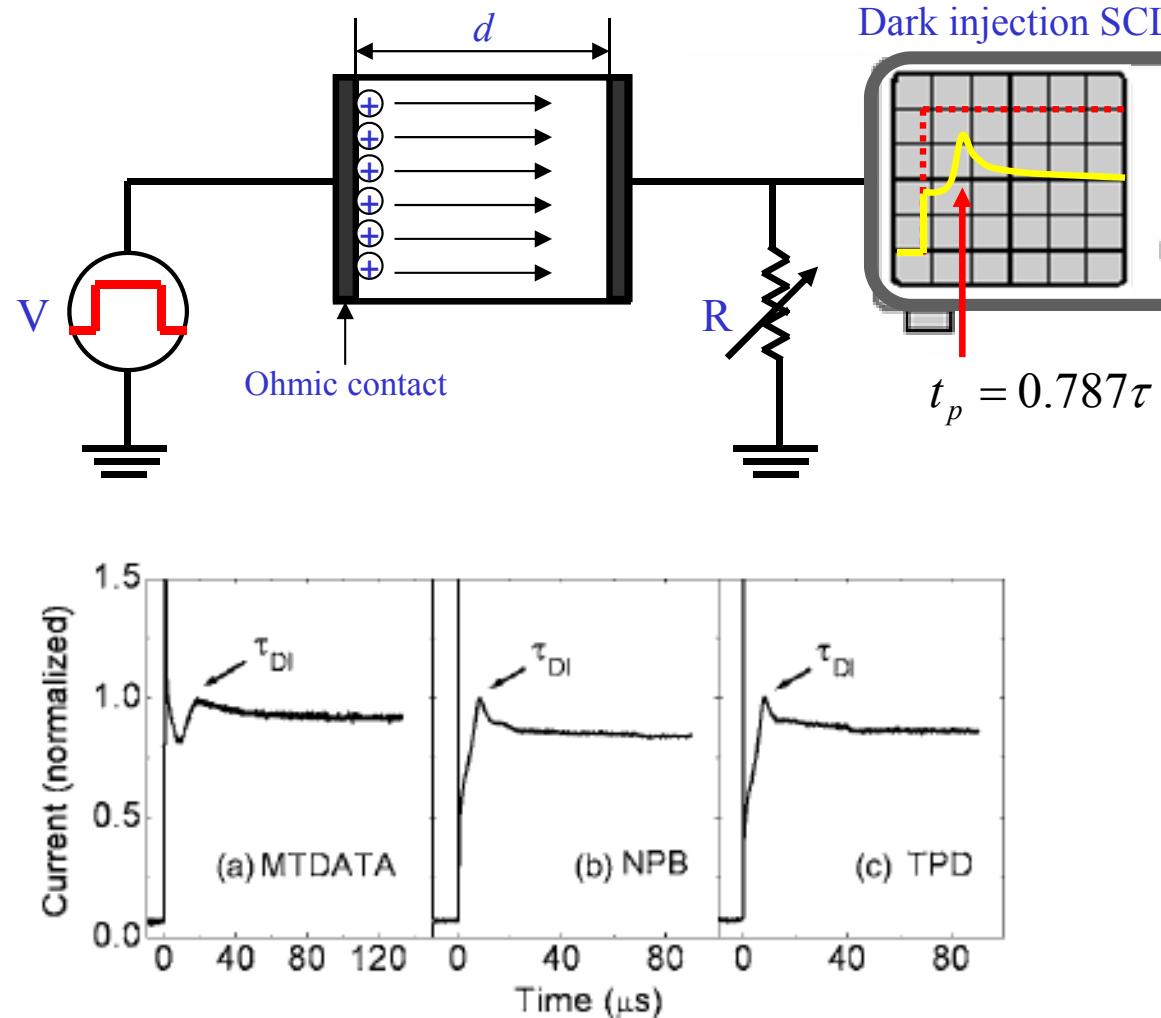
Mobility Measurement Techniques



Other mobility measurement techniques

- Dark injection in the space-charge limited current regime
 - I-V characteristics of space charge limited current
 - Transient EL
 - SHG measurement [T. Manaka, E. Lim, R. Tamura, M. Iwamoto, *Nature Photon.* **1**, 581–584 (2007).]
-

Transient SCLC



Dark injection SCLC transient current

$$t_p = 0.787\tau$$

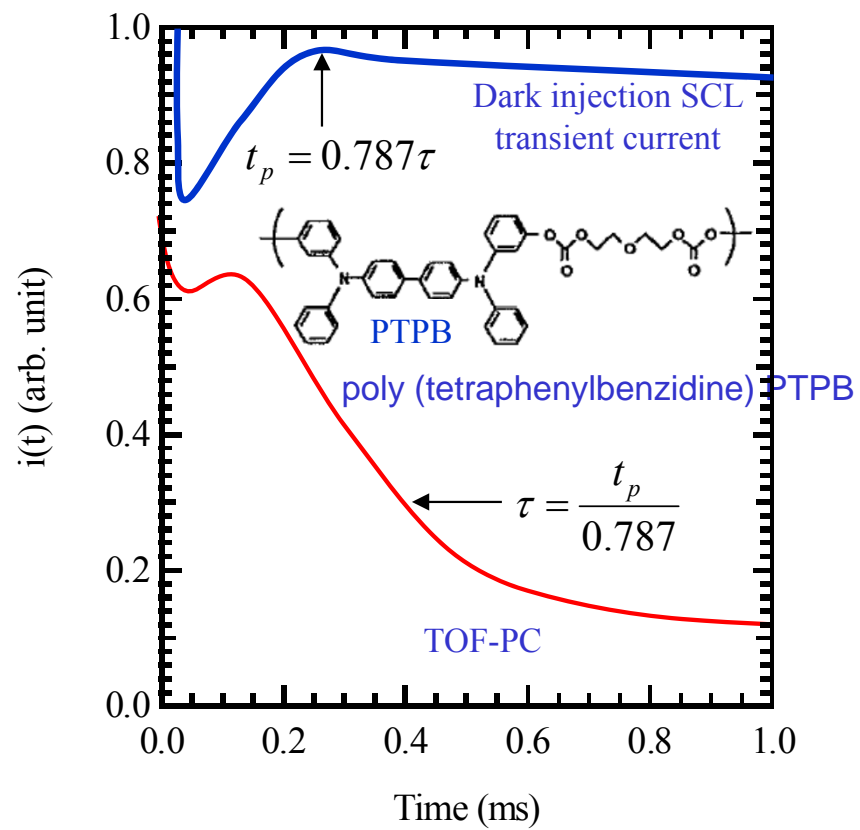


FIG. 5. Room temperature DI signals for MTDATA, NPB, and TPD under applied field strengths of 0.10, 0.09, and 0.09 MV/cm, respectively. The film thicknesses for MTDATA, NPB, and TPD were 0.76, 4.11, and 5.13 μm , respectively.

S.C. Tse, S.W. Tsang, and S.K. So, J. Appl. Phys. 100, 063708 (2006).

M. Abkowitz, J. S. Facci, and M. Stolka, Appl. Phys. Lett. 63, 1892 (1993).



Mobility Measurement Techniques: dark charge injection

In a monopolar and single-layer configuration, the carrier transit time is shorter than in the absence of space-charge effects due to the enhancement of the electric field at the leading edge of the carrier packet.

$$t_{tr} = 0.786 \frac{d}{\mu E}$$

The transient current overshoots its steady-state value by a factor of 1.21 and starts at 0.44 times the steady-state value.

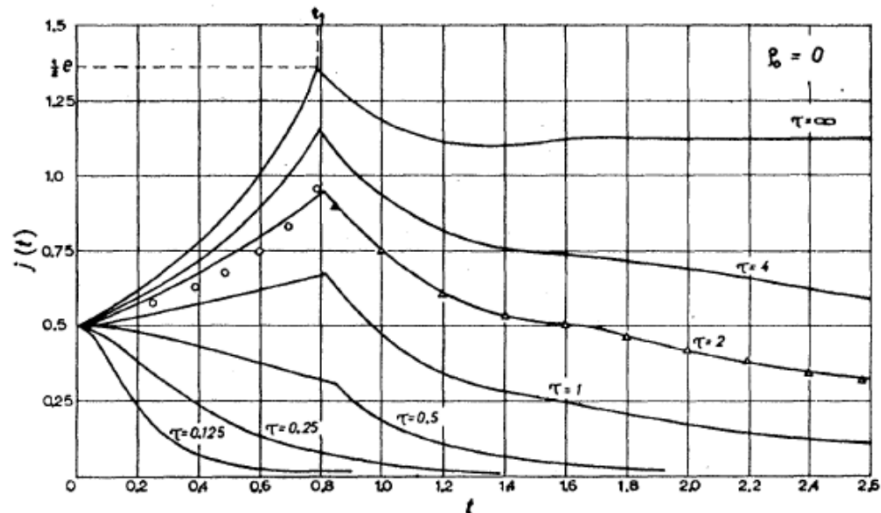
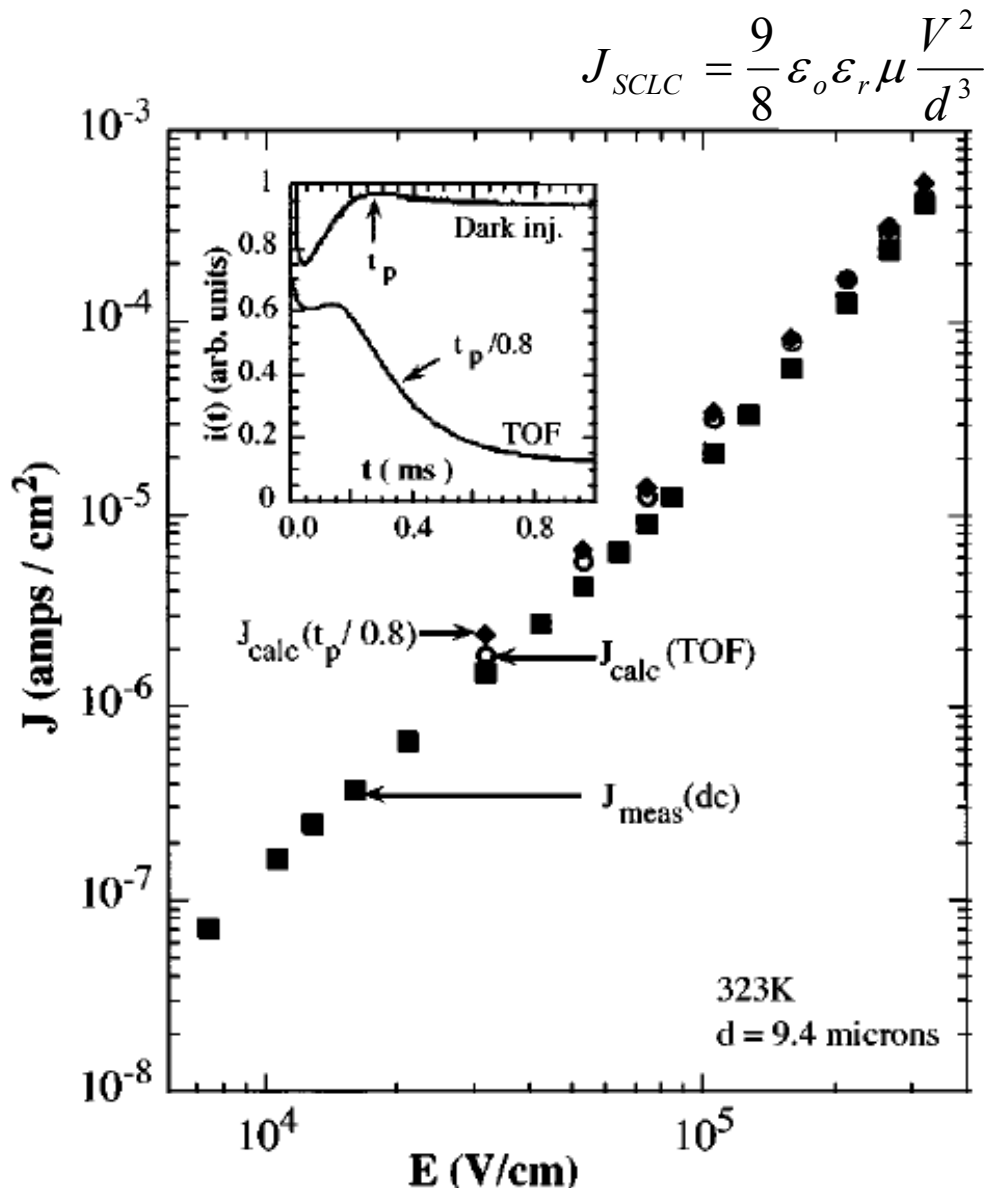


FIG. 5. The time dependence of the SCLC density for insulating crystals characterized by various trapping times, and $\theta_0 = 0$.

A. Many and G. Rakavy, Phys. Rev. **126**, 1980 (1962)



M. Abkowitz, J. S. Facci, J. Rehm, J. Appl. Phys. 1998, 83, 2670.

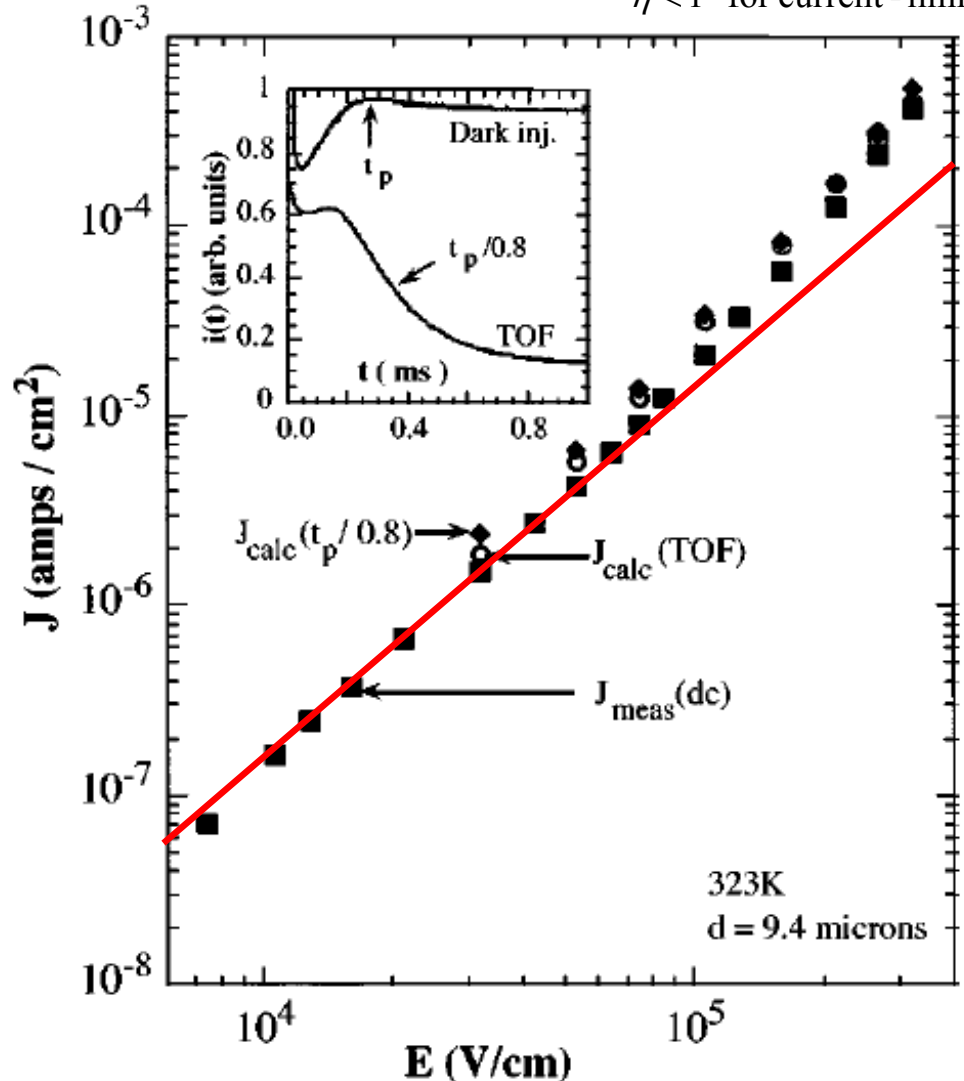
Carrier injection efficiency

$$J_{SCLC} = \frac{9}{8} \frac{\varepsilon_o \varepsilon_r \mu V^2}{d^3}$$

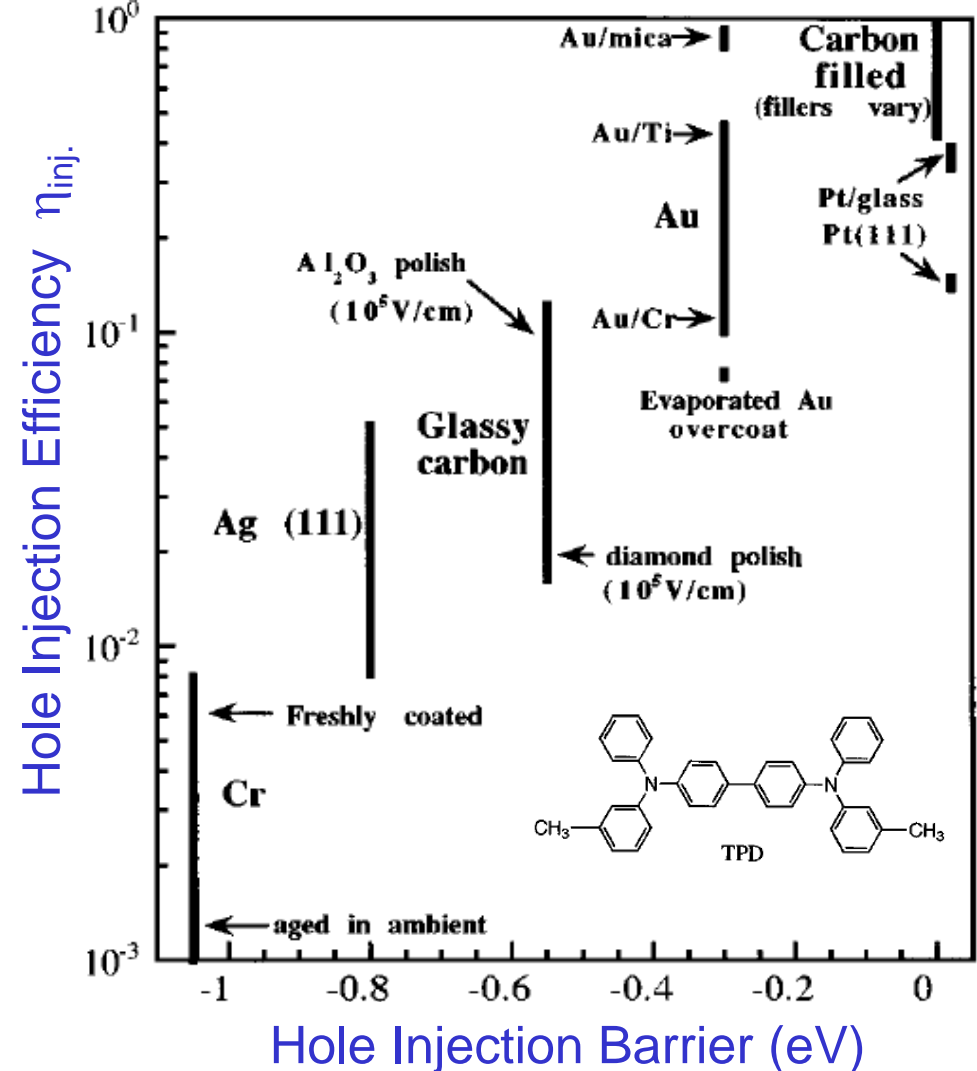
Injection efficiency: $\eta = \frac{\text{injected current}}{\text{SCLC}}$

$\eta = 1$ for ohmic contact

$\eta < 1$ for current - limiting contact

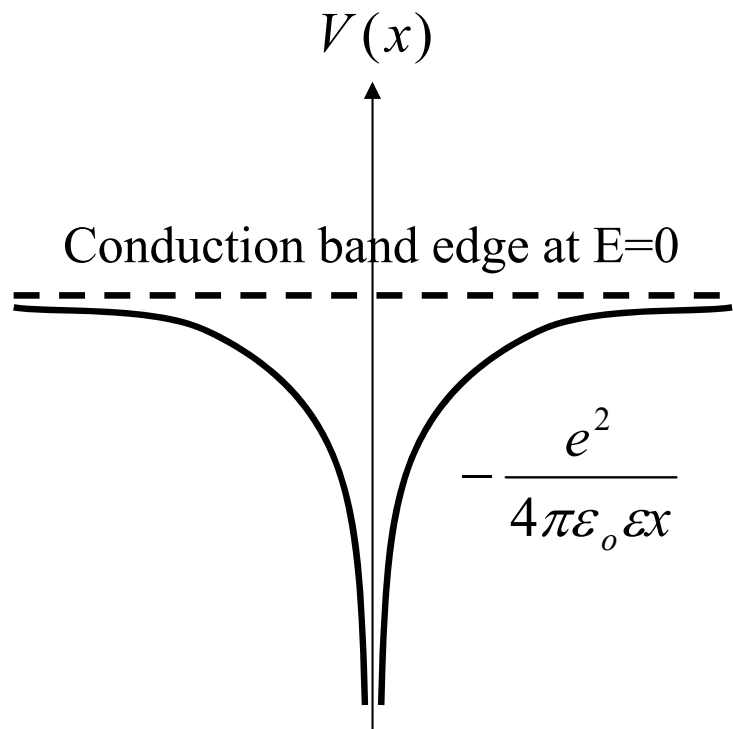


M. Abkowitz, J. S. Facci, J. Rehm, J. Appl. Phys. 1998, 83, 2670.

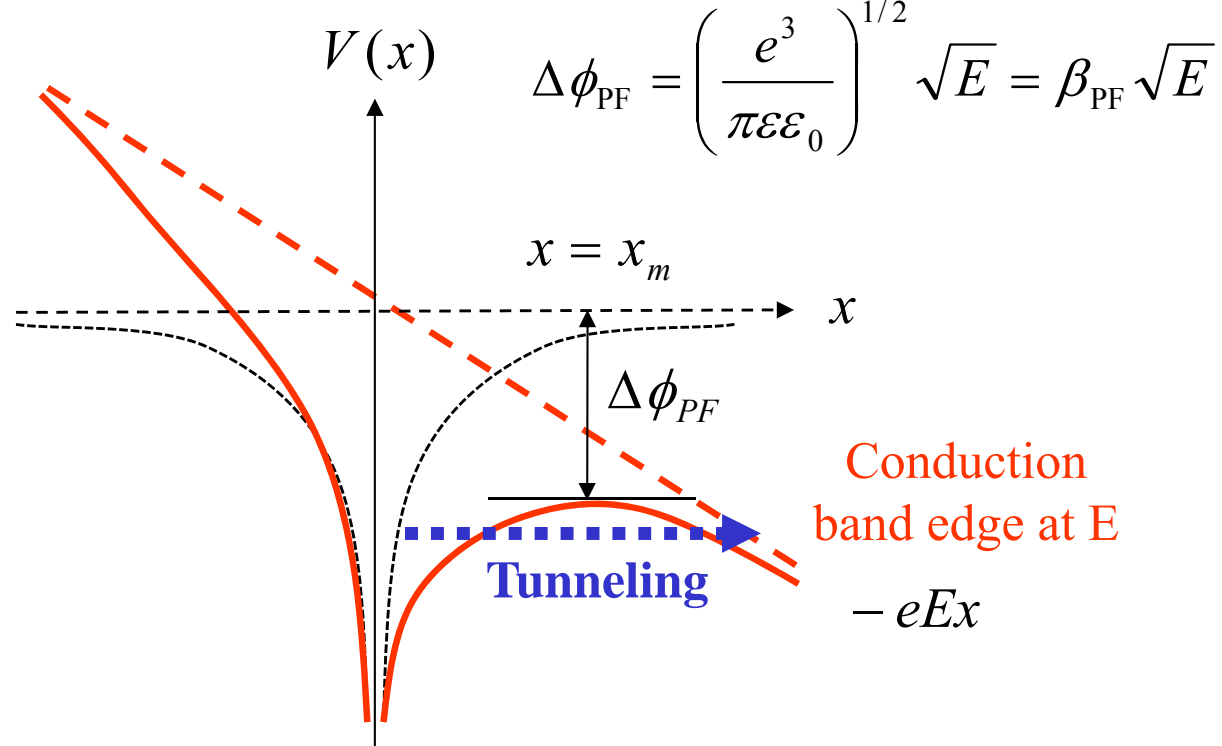


Charge Transport in Disordered Organic Solids

(1) Poole-Frenkel Model



Zero field ($E=0$)



$E \neq 0$

$$\mu(F, T) = \mu_{PF} \exp\left(-\frac{\Delta E}{k_B T}\right) \exp\left(\frac{\beta_{PF} \sqrt{E}}{k_B T}\right)$$

$$\beta_{PF} = \sqrt{\frac{e^3}{\pi\epsilon\epsilon_0}}$$

ΔE : Activation energy at $E=0$

μ_{PF} : PF Mobility

β_{PF} : PF constant

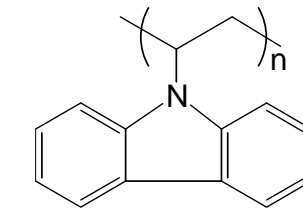
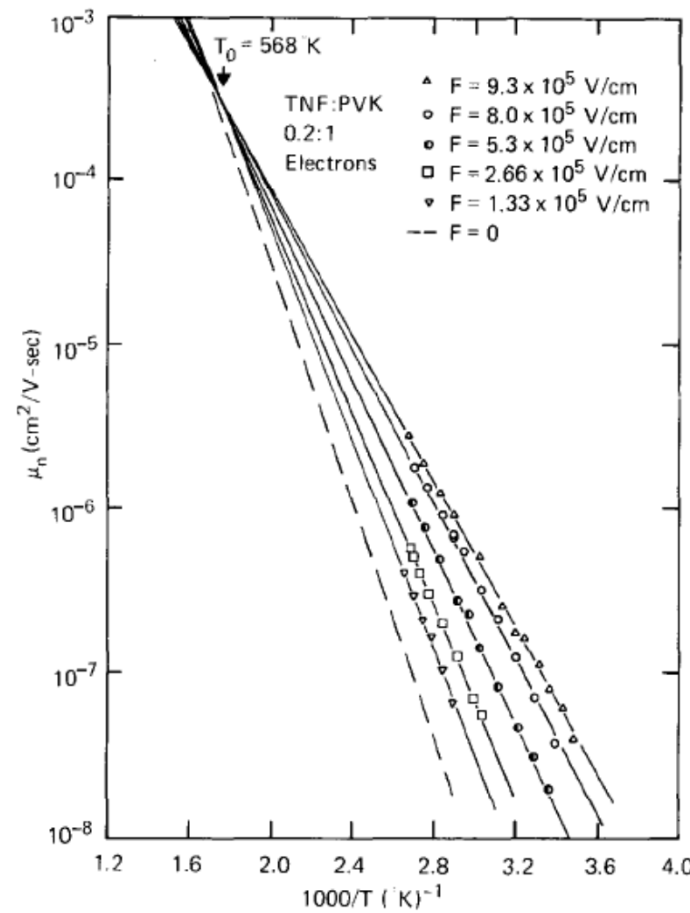
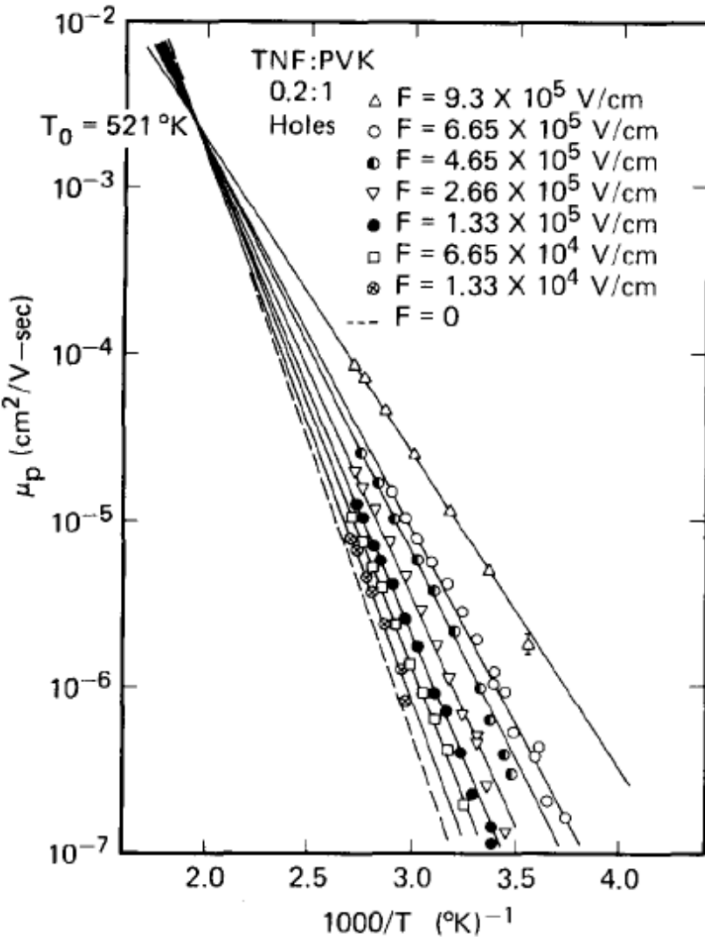


Charge Transport in Disordered Organic Solids

(2) Gill's modified Poole-Frenkel model

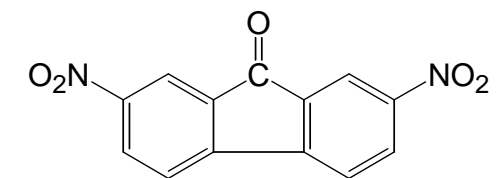
$$\mu(F, T) = \mu_{\text{PF}} \exp\left(-\frac{\Delta E}{k_B T_{\text{eff}}}\right) \exp\left(\frac{\beta_{\text{PF}} \sqrt{E}}{k_B T_{\text{eff}}}\right) \quad \frac{1}{T_{\text{eff}}} = \frac{1}{T} - \frac{1}{T_0}$$

T_0 : Empirical parameter



PVK

poly-n-vinylcarbazole
(hole conductor)



TNF

2,4,6-trinitro-9-fluorenone
(electron acceptor)

W. D. Gill, J. Appl. Phys. **43**, 5033 (1972).

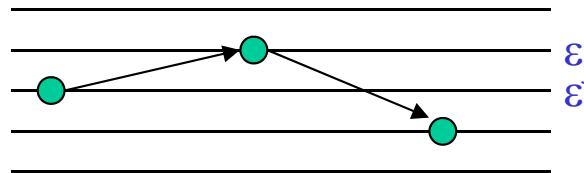


Charge Transport in Disordered Organic Solids

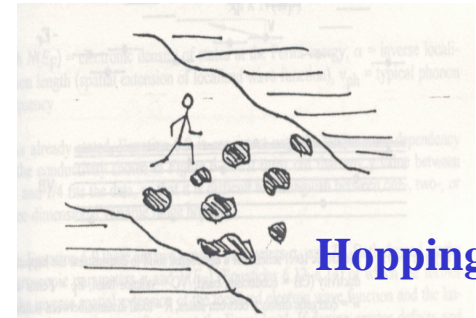
(3) Bassler's Gaussian Disorder Model

- The energy of each site is distributed in accordance with the Gaussian distribution
- Energies of adjacent sites are uncorrelated and motion between sites is Markovian (no phase memory)
- The transition rates for phonon-assisted tunneling (Miller and Abrahams):

$$W_{ij} = v_{ph} \exp(-2\alpha R_{ij}) \begin{cases} \exp\left(-\frac{\epsilon_i - \epsilon_j}{kT}\right), & \epsilon_i > \epsilon_j \\ 1, & \epsilon_i < \epsilon_j \end{cases}$$



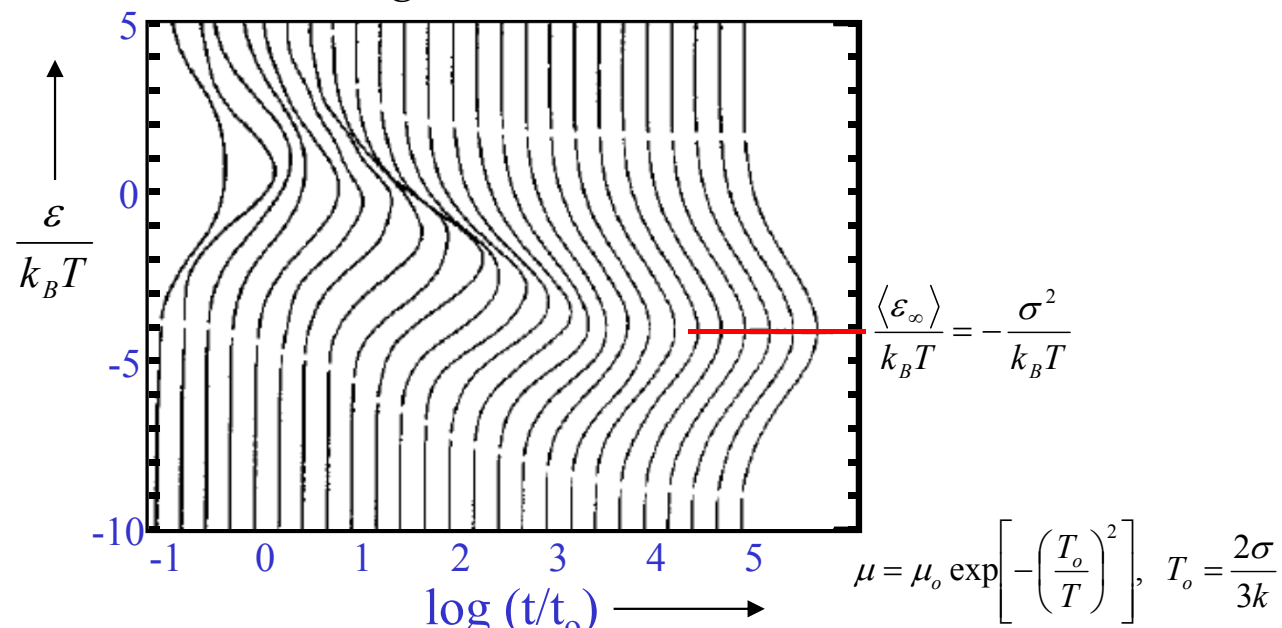
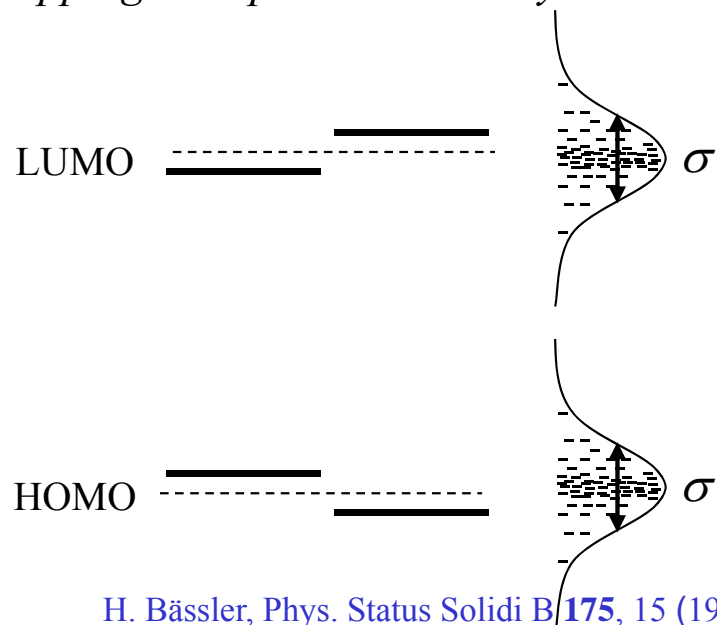
A. Miller, E. Abrahams, Phys. Rev. **120** (1960) 745.



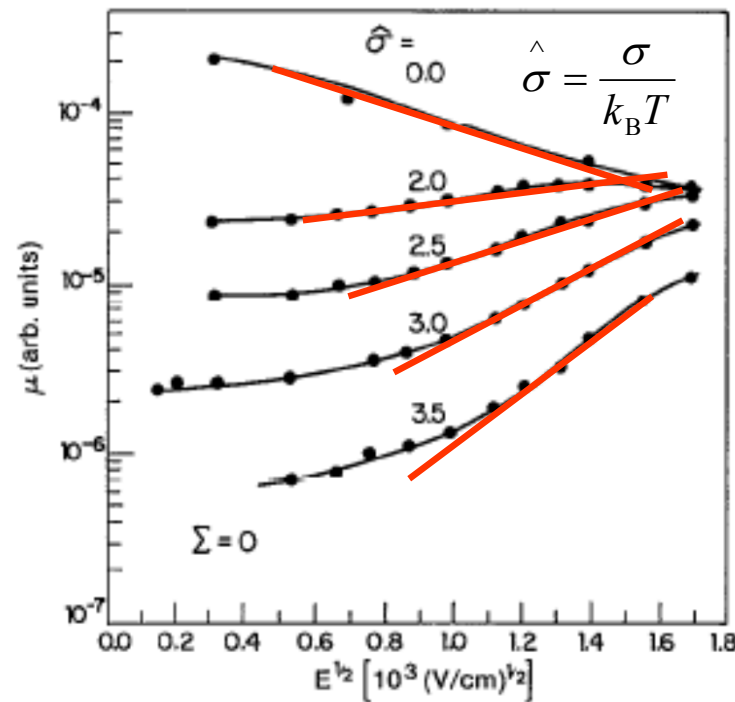
Hopping

α = inverse localization length, R_{ij} = distance between the localized states, ϵ_i = energy at the state i.

- Since the hopping rates are strongly dependent on both the positions and the energies of the localized states, *hopping transport is extremely sensitive to structural as well as energetic disorder.*



Bassler's Gaussian Disorder Model



σ : Energetic disorder

Σ : Positional disorder

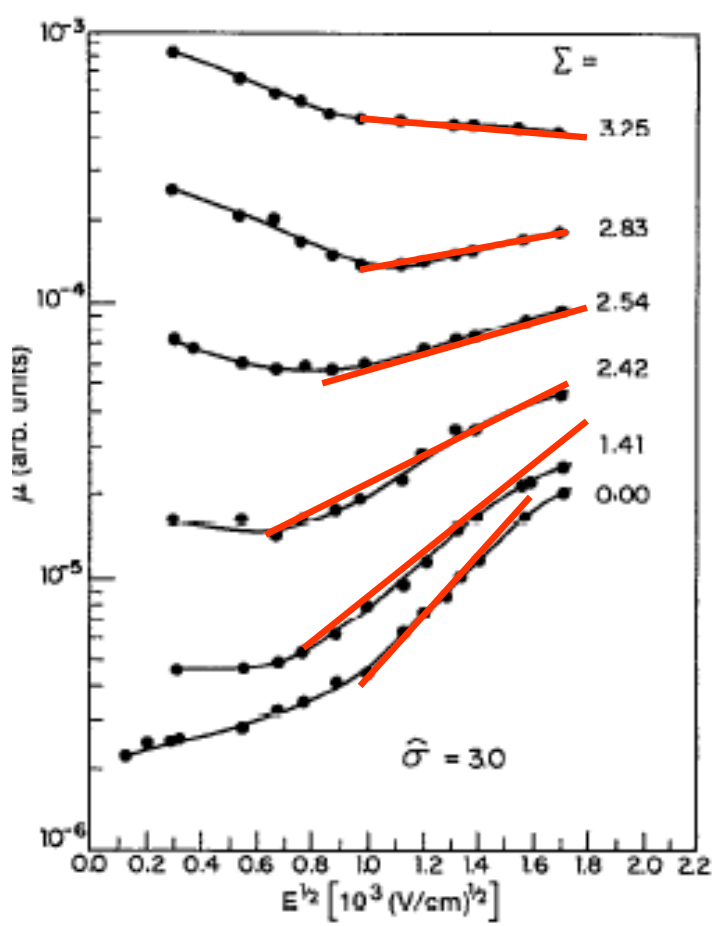
C : Constant $\sim 2.9 \times 10^{-4}$ $(\text{cm}/\text{V})^{1/2}$

μ_o : High temperature limit of the mobility

$$\mu(E, T) = \mu_o \exp \left[- \left(\frac{2\sigma}{3k_B T} \right)^2 \right] \exp \left\{ C \left[\left(\frac{\sigma}{k_B T} \right)^2 - 2.25 \right] \sqrt{E} \right\}, \quad (\Sigma \leq 1.5)$$

$$\mu(E, T) = \mu_o \exp \left[- \left(\frac{2\sigma}{3k_B T} \right)^2 \right] \exp \left\{ C \left[\left(\frac{\sigma}{k_B T} \right)^2 - \Sigma^2 \right] \sqrt{E} \right\}, \quad (\Sigma > 1.5)$$

H. Bassler, Phys. Status Solidi B **175**, 15 (1993).

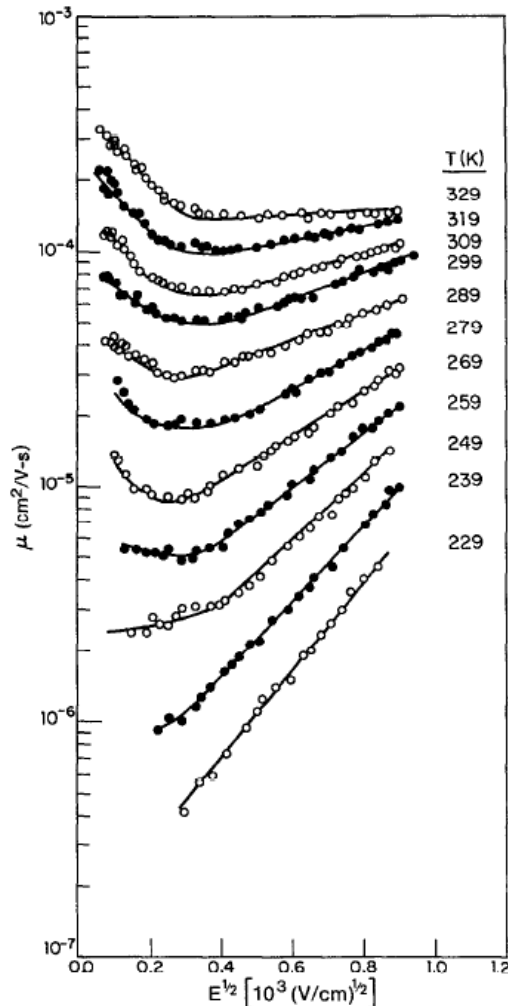
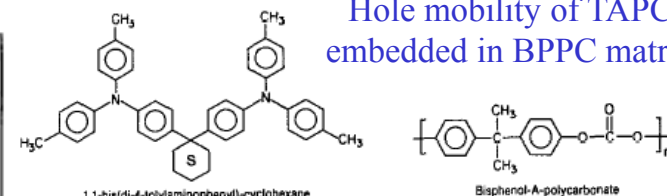


$$\mu_o(\rho) = a_o \rho^2 \exp(-2\rho/\rho_o),$$

where ρ = average inter-site distance
and ρ_o = carrier localization radius

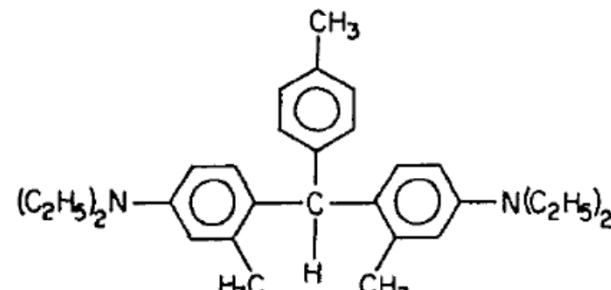
M. Stolka, J. F. Janus and D. M. Pai,
J. Phys. Chem. **88**, 4707 (1984).

Hole mobility of TAPC
embedded in BPPC matrix

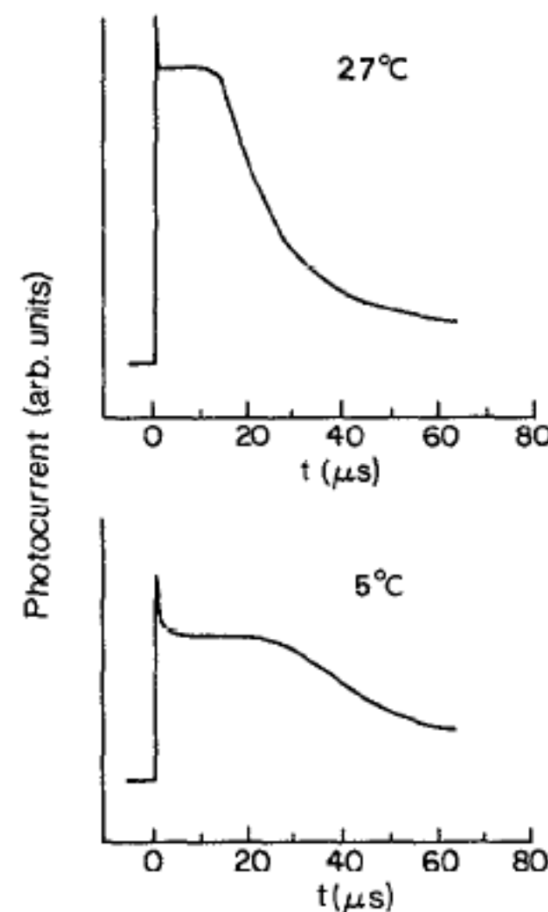


P. M. Borsenberger, L. Pautmeier and H. Bassler,
J. Chem. Phys. **94**, 5447 (1991).

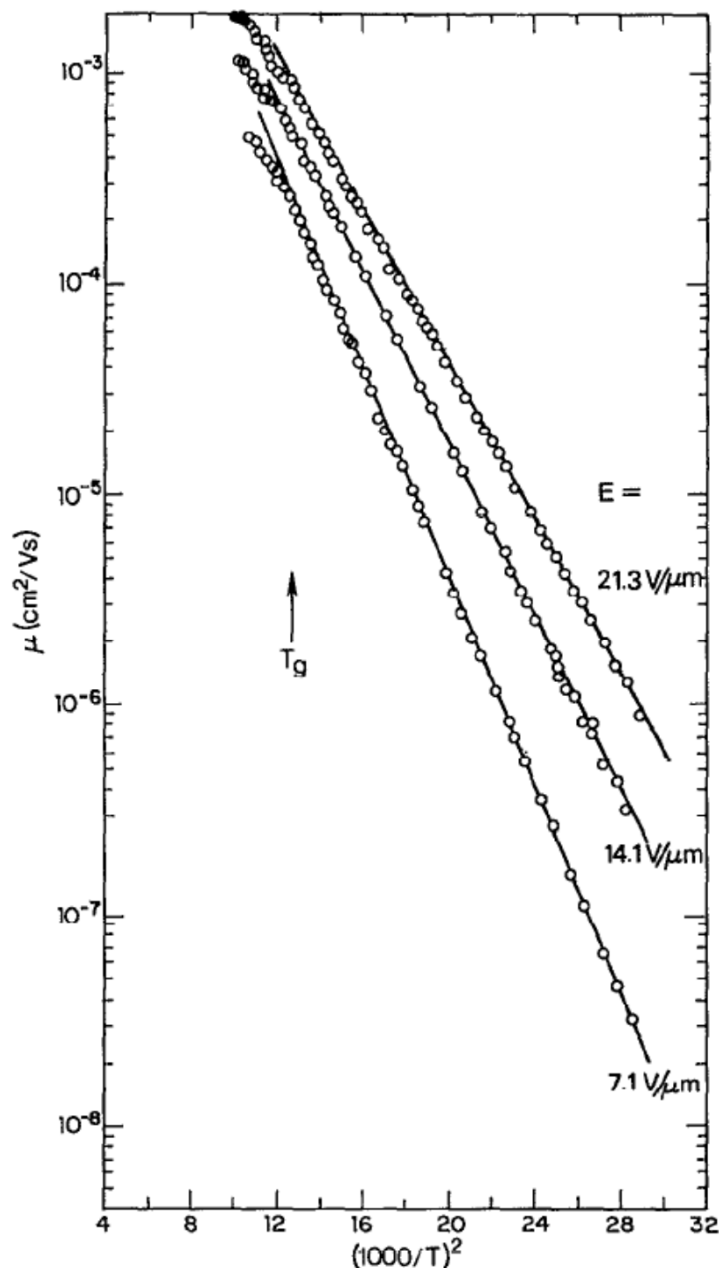
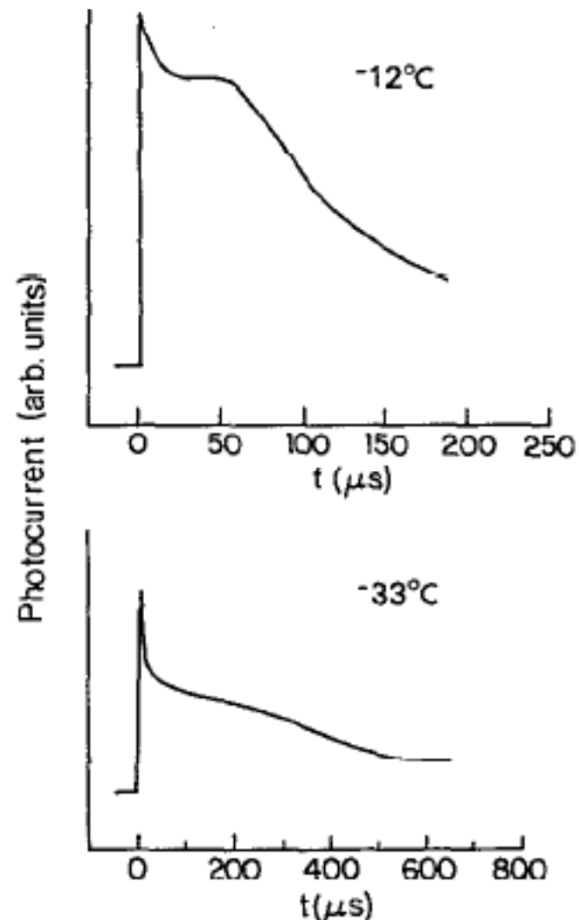
Charge Transport in Disordered Polymers



Hole mobility of MPMP



MPMP
bis(4-N,N-diethylamino-2-methylphenyl)-4-methylphenylmethane
(thickness~8.7 μm)



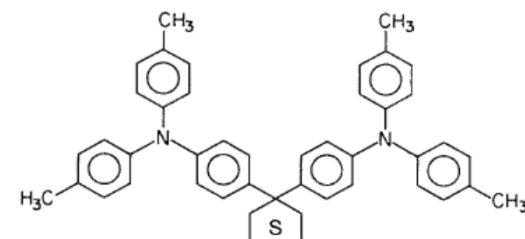
P. M. Borsenberger, L. Pautmeier and H. Bässler, J. Chem. Phys. **95**, 1258 (1991)



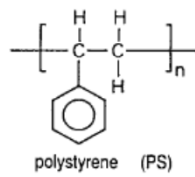
Disorder parameters

Disorder parameters

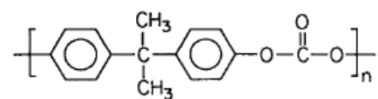
- σ : The width of the DOS. Random distribution of both permanent and van der Waals dipoles lead to local fluctuations in electric potential → increase σ by an amount proportional to the square root of the dipole concentration and to the strength of the dipole moment. → reduce the carrier mobility. The smaller dipolar interaction is better for the carrier transport.
- Σ : The degree of positional disorder. Amorphous morphology of molecular solids or doped polymers lead to the variation in the intermolecular distances.



(a) 1,1-bis(di-4-tolylaminophenyl)-cyclohexane (TAPC)



(b)



(c)

FIG. 1. Molecular structures of compounds used in this study.

P. M. Borsenberger and H. Bässler, J. Chem. Phys. **95**, 5327 (1991).

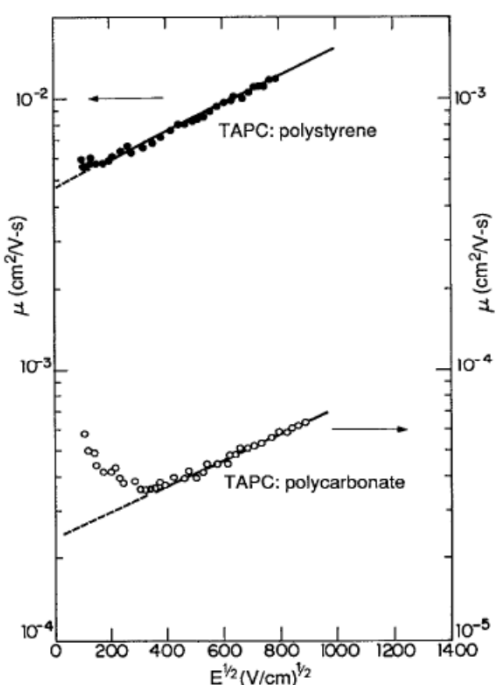


FIG. 2. Logarithm of the mobility vs $E^{1/2}$ for TAPC doped polystyrene and TAPC doped polycarbonate measured at 295 K.

$\mu_{\text{TAPC doped polystyrene}} \gg \mu_{\text{TAPC doped polycarbonate}}$

Dipole moment:

- TAPC [1,1-bis(di-4-tolylaminophenyl)cyclohexane] = 1.0 D
- PC (bisphenol-A-polycarbonate) = 1.0 D
- PS (polystyrene) = 0.1 D

- Larger dipolar interaction increases both σ and Σ .
- The elimination of random dipolar fields due to static dipole moments of PC reduces both σ and Σ and thereby increases the mobility.

Influence of impurity on the carrier mobility

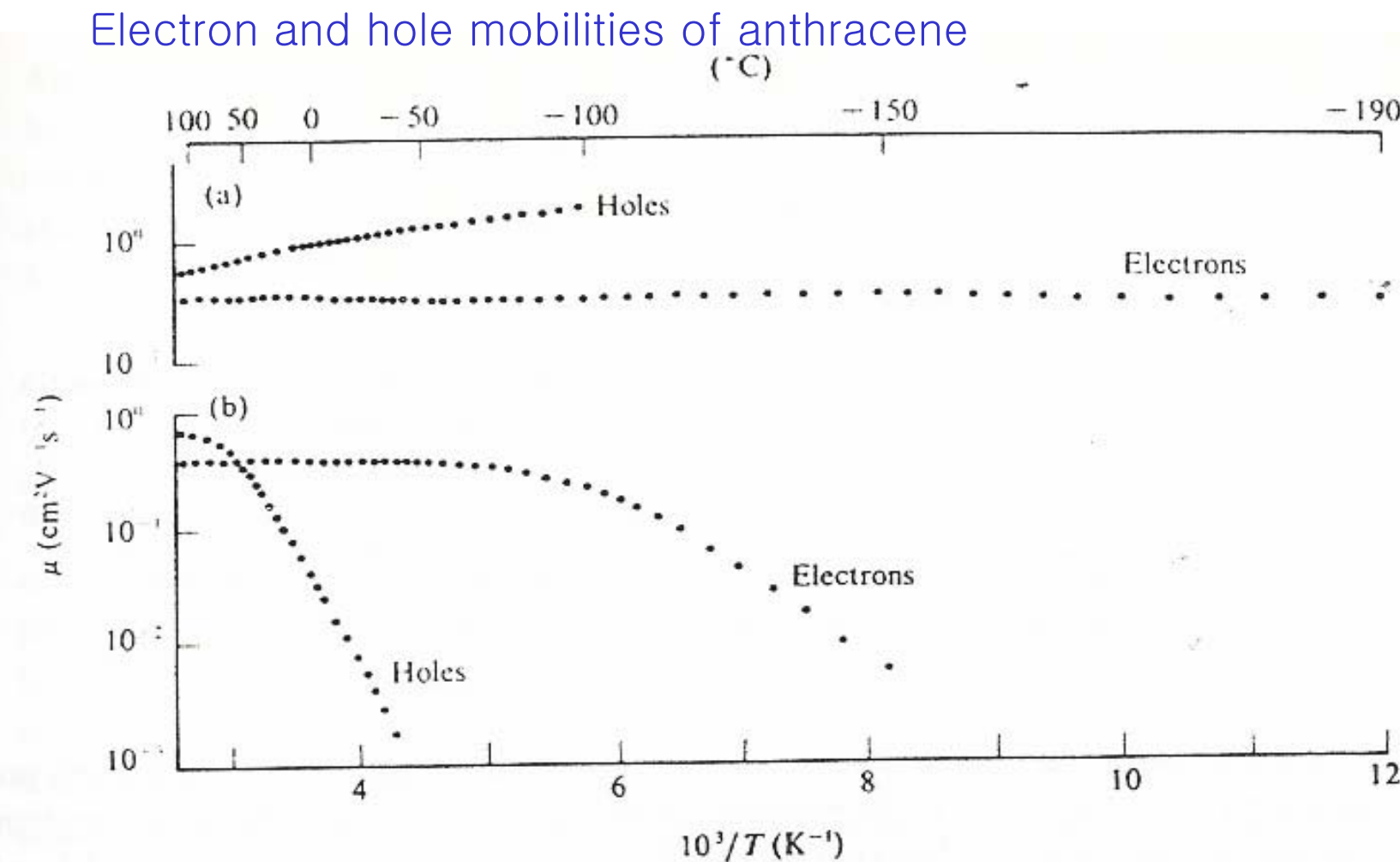
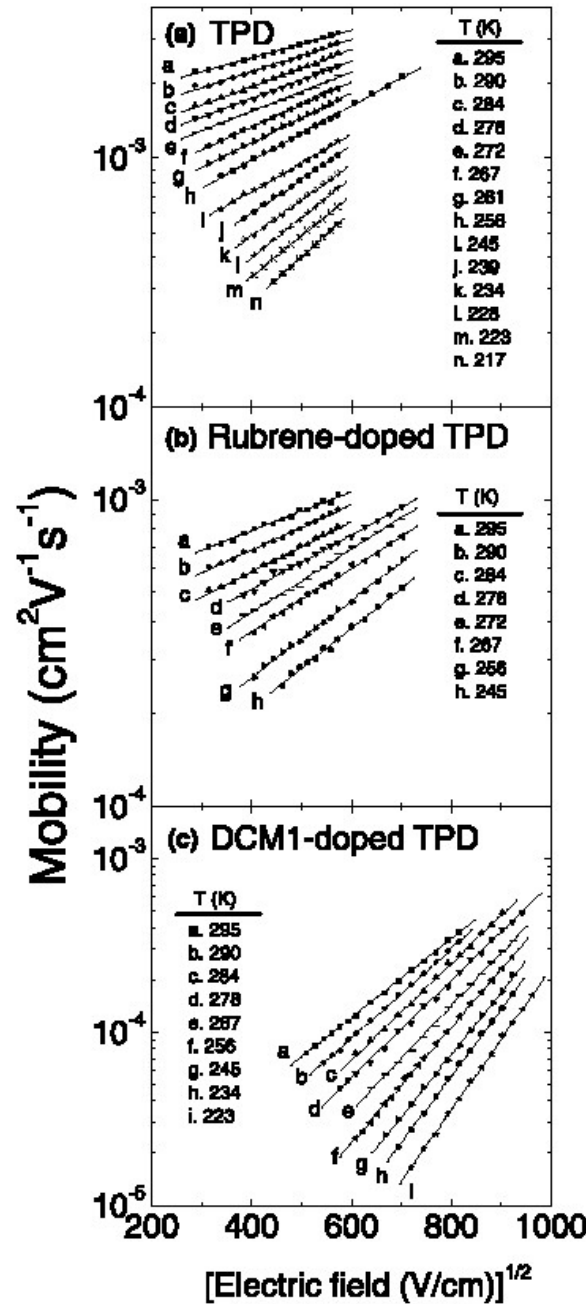
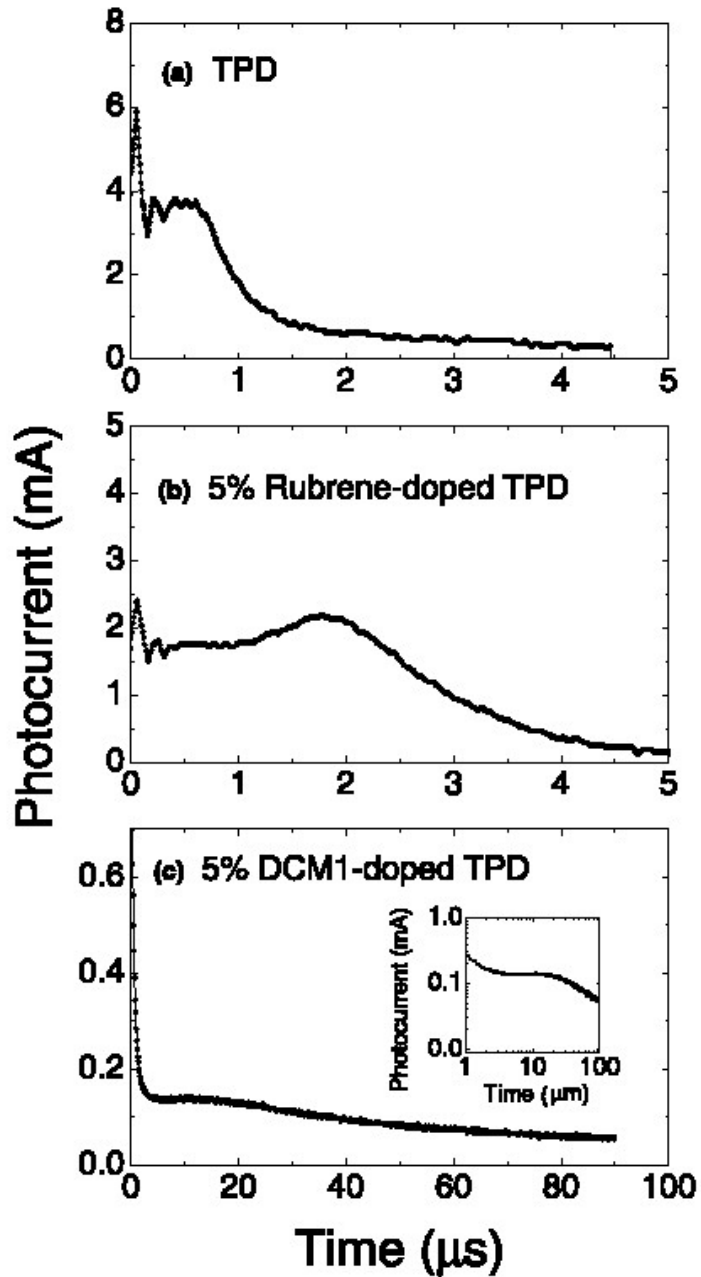


Fig. II.F.14. The influence of 10^{-7} mol/mol tetracene doping on the anthracene c' charge carrier mobilities. (a) Undoped crystal mobilities; (b) doped crystal mobility. Note the asymmetry between the hole and electron trapping, and the trap depths calculated using Eq. II.F.2.32. (Karl 1980a)

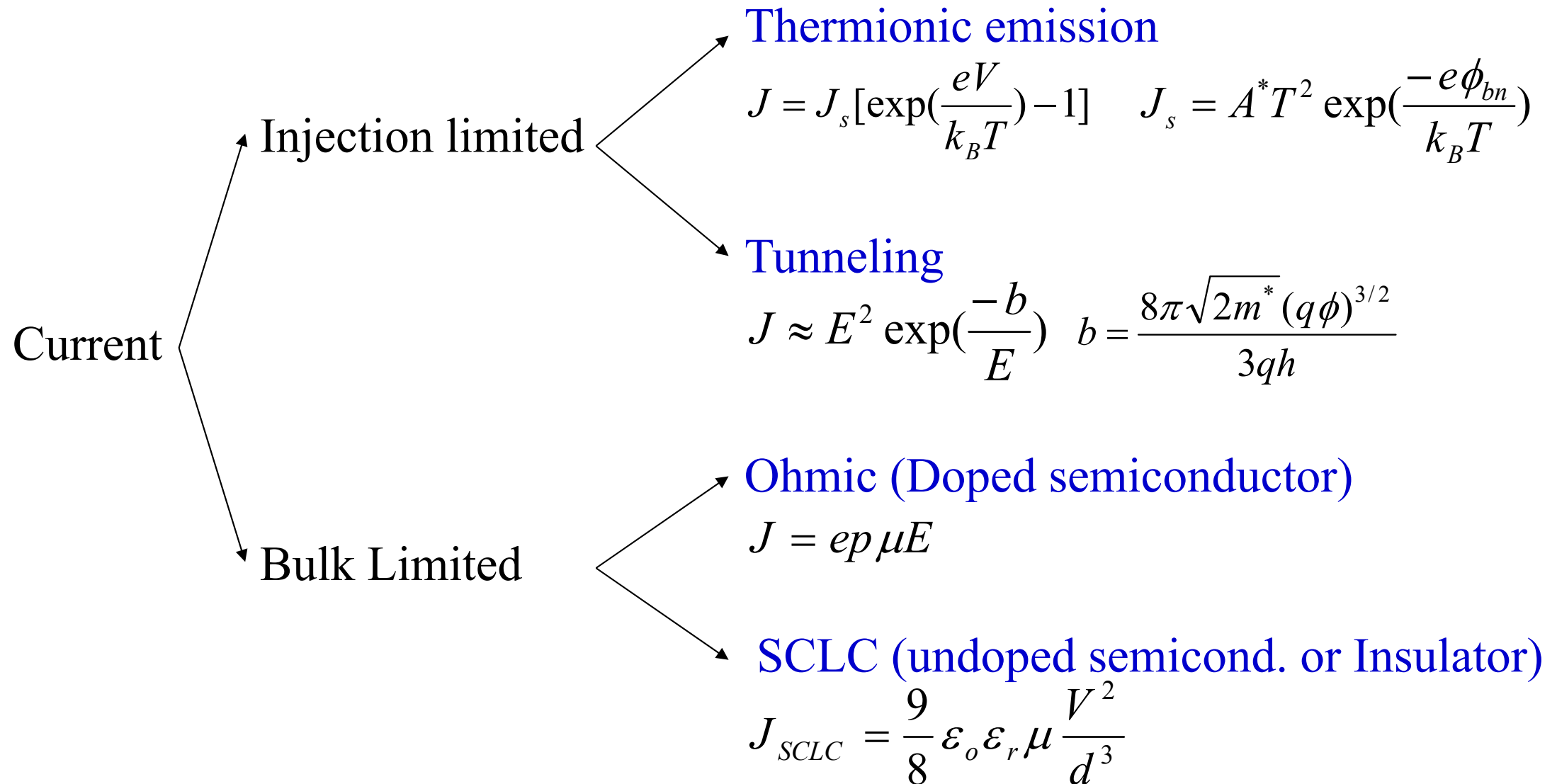
Mobility – Doping Relation



Doping reduces carrier mobility and affects I-V-EL characteristics.

Ref. H.H. Fong et al.
Chem. Phys. Lett. 353 (2002) 407

Charge –voltage characteristics of organic semiconductors



Carrier injection at the contact

Thermionic Emission

$$J = J_s \left[\exp\left(\frac{eV}{nk_B T}\right) - 1 \right]$$

$$J_s = A^* T^2 \exp\left(\frac{-e\phi_{bn}}{k_B T}\right)$$

*effective Richardson constant
for thermionic emission*

$$A^* = \frac{4\pi e m_n^* k_B}{h^3} = 120 \left(\frac{m^*}{m} \right) \text{ A/cm}^2/\text{K}^2$$

Fowler-Nordheim Tunneling

$$J_s \approx E^2 \exp\left(\frac{-b}{E}\right) \quad b = \frac{8\pi\sqrt{2m^*}(q\phi)^{3/2}}{3qh}$$

Schottky effect $\Delta\Phi = \sqrt{\frac{e^3 F}{4\pi\epsilon\epsilon_0}}$

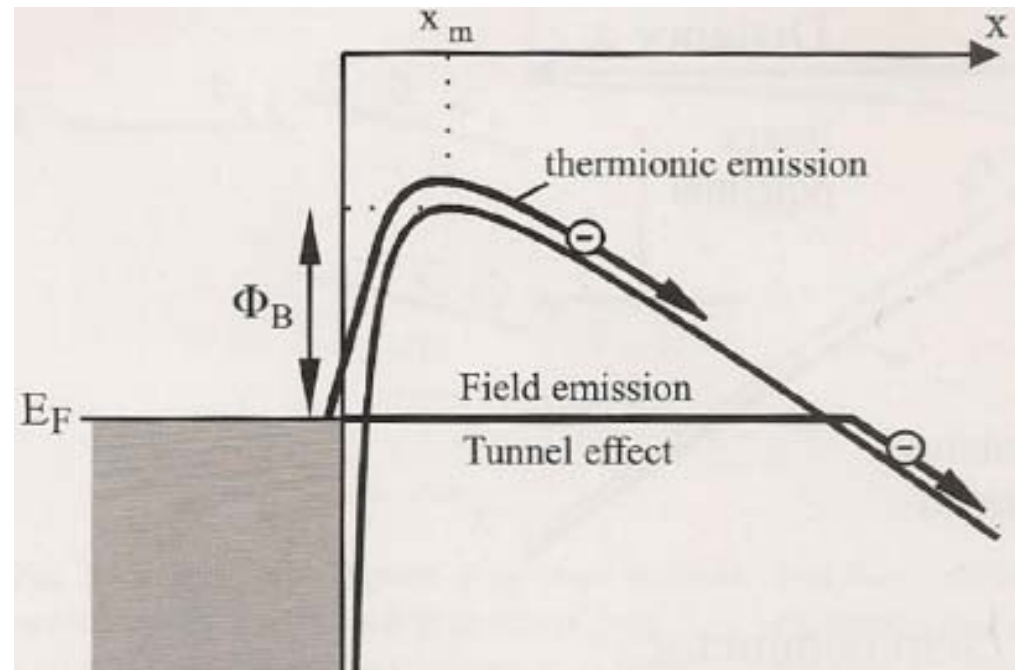


Fig. 8.24 Thermionic emission and field emission.

Carrier Injection : Fowler-Nordheim Tunneling

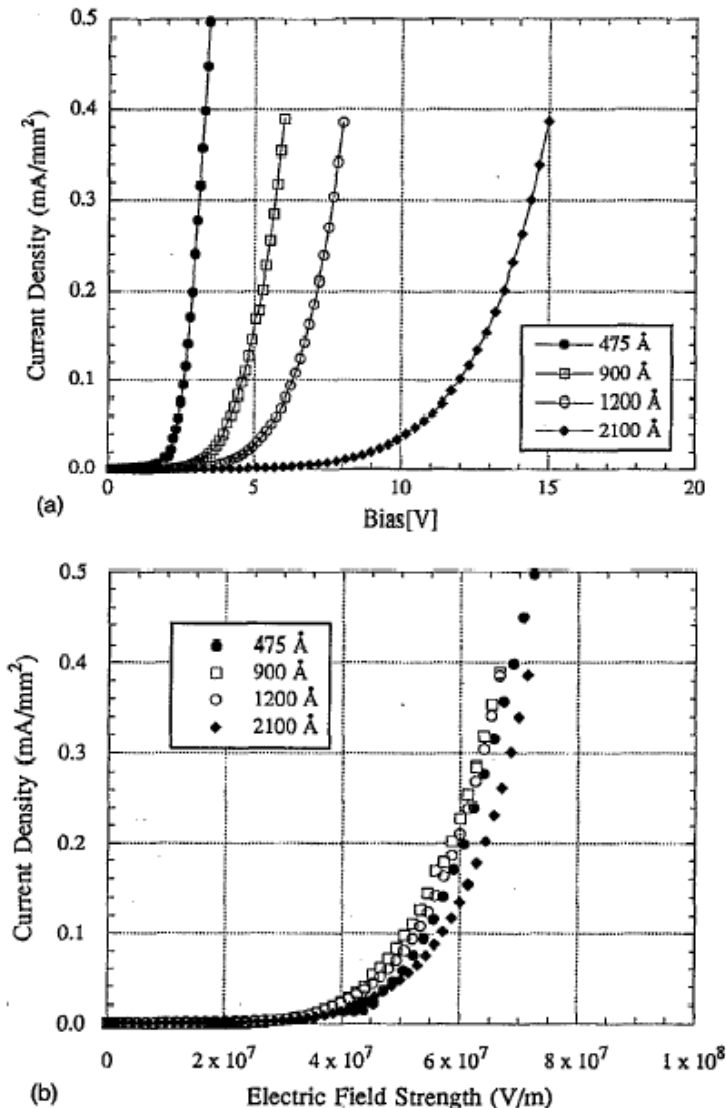


FIG. 2. (a) Thickness dependence of the I - V characteristics in an ITO/MEH-PPV/Ca device. (b) Electric field ν current dependence for the above devices.

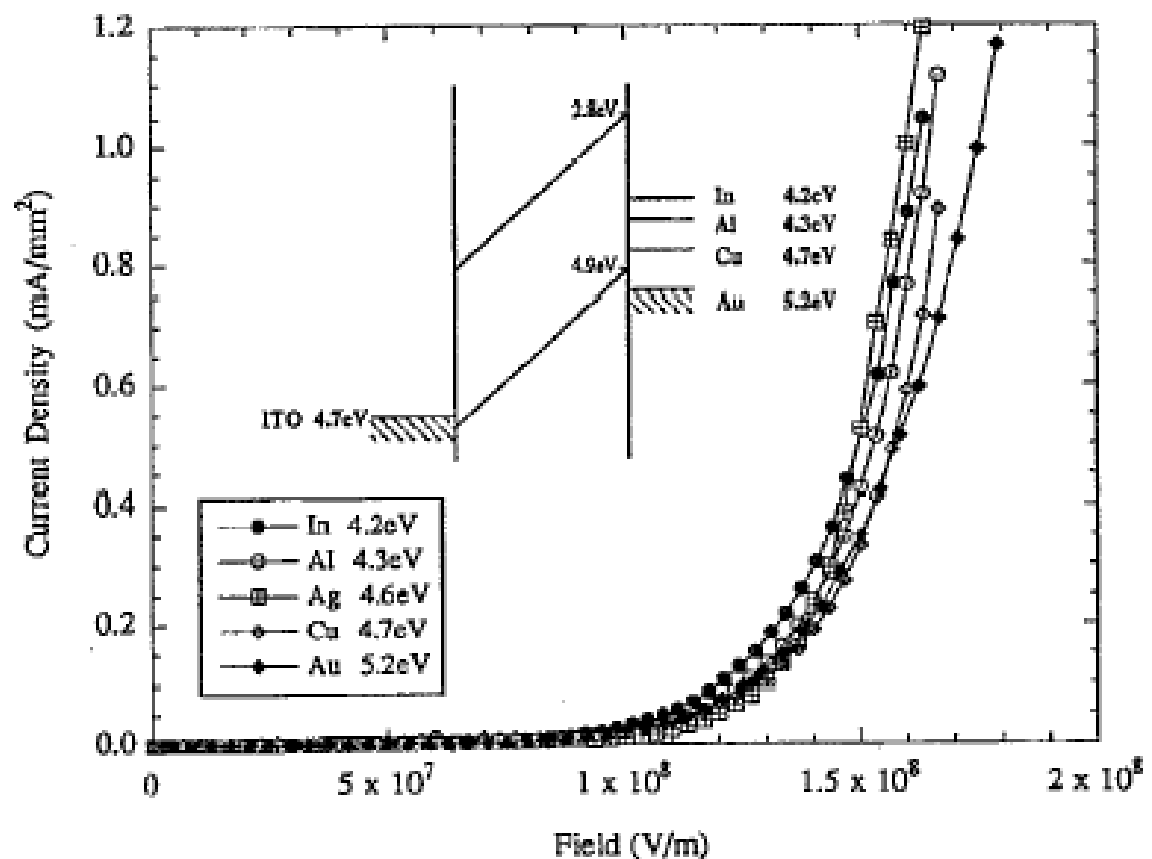


FIG. 3. I - V characteristics of 1200 Å thick “hole-only” devices. Inset shows band models indicating the relative position of the Fermi energies of the various materials.

I. D. Parker, J. Appl. Phys. **75**, 1656 (1994).

Carrier Injection : Fowler-Nordheim Tunneling

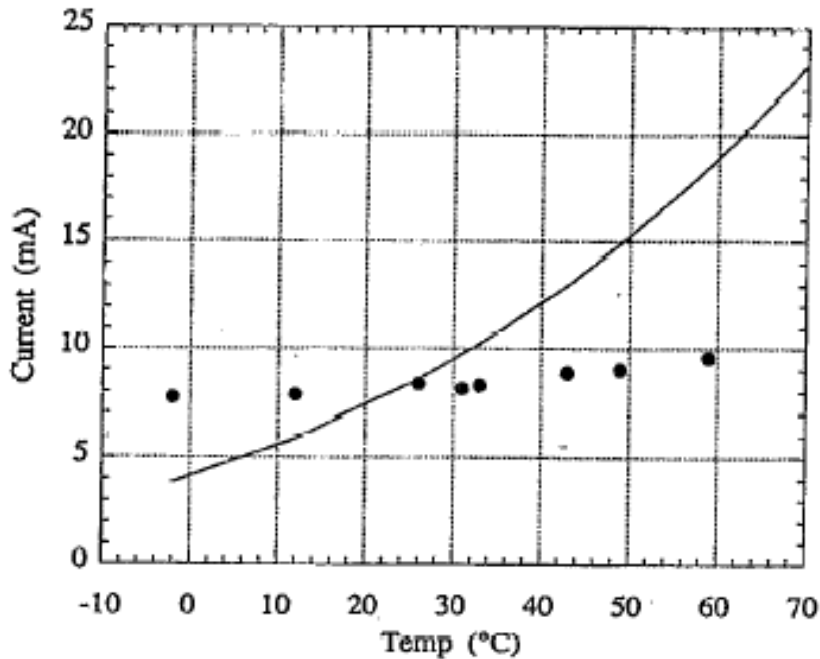


FIG. 5. Temperature dependence of a 1200 Å thick ITO/MEH-PPV/Au device operating at 17 V bias. For comparison, the solid line indicates the I - V characteristics of a 0.2 eV Schottky barrier device.

Fowler-Nordheim Tunneling

$$J_s \approx E^2 \exp\left(\frac{-b}{E}\right)$$

$$b = 8\pi(2m^*)^{1/2} (q\Phi)^{3/2} / 3qh$$

I. D. Parker, J. Appl. Phys. **75**, 1656 (1994).

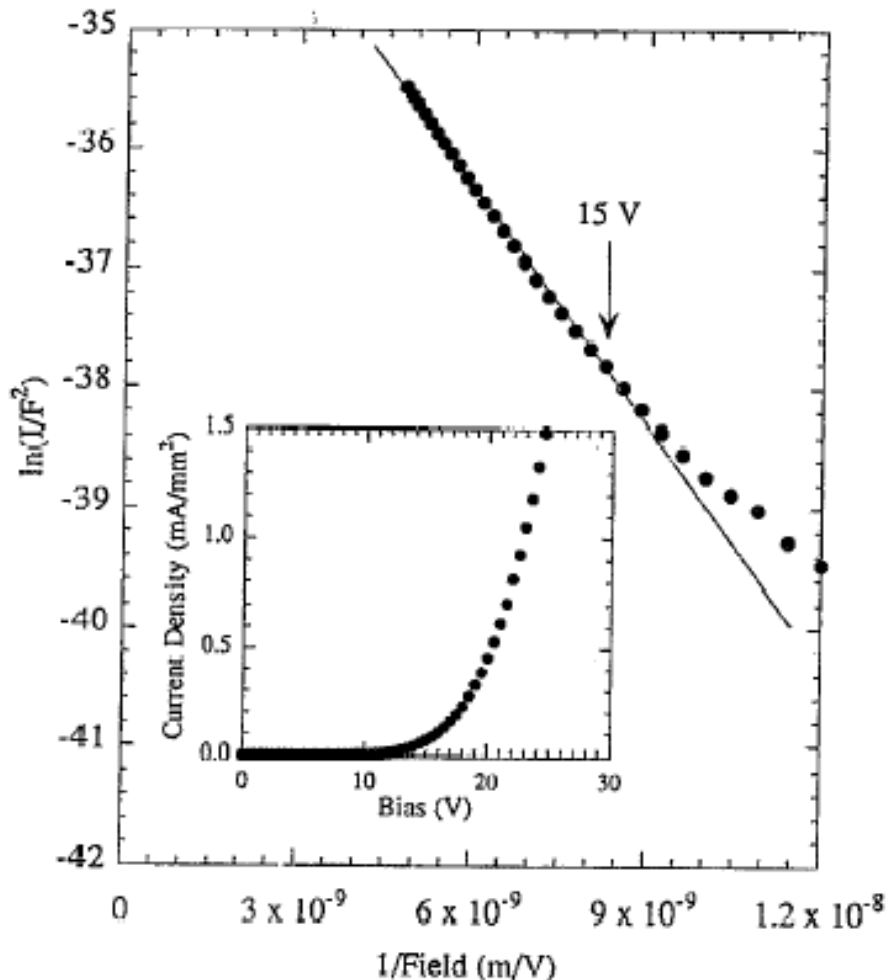
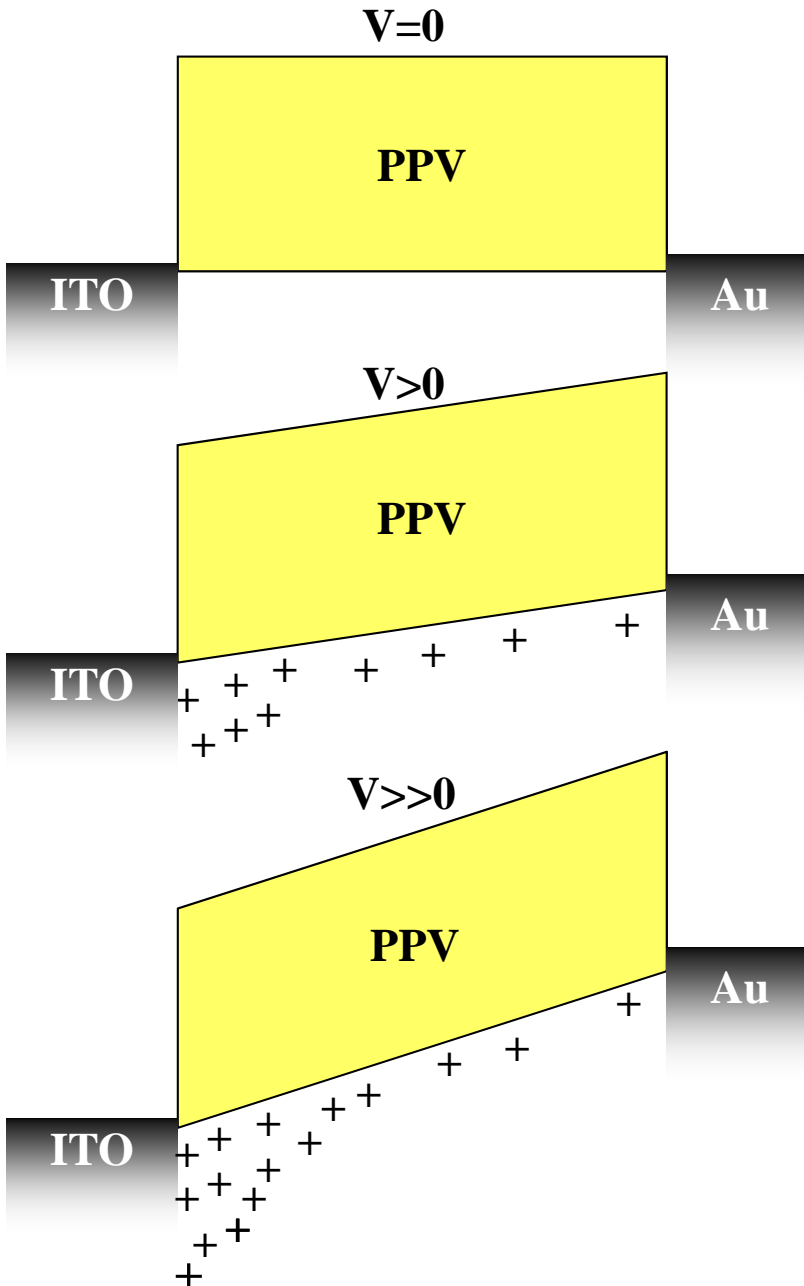


FIG. 6. Fowler-Nordheim plot for a 1200 Å thick ITO/MEH-PPV/Au device. Inset shows the I - V characteristics of the device.

Space-charge-limited current (SCLC)



Space-charge-limited current (SCLC)

OLED acts as a capacitor

$$J_{SCLC} \approx (\text{charge density}) \times \text{velocity}$$

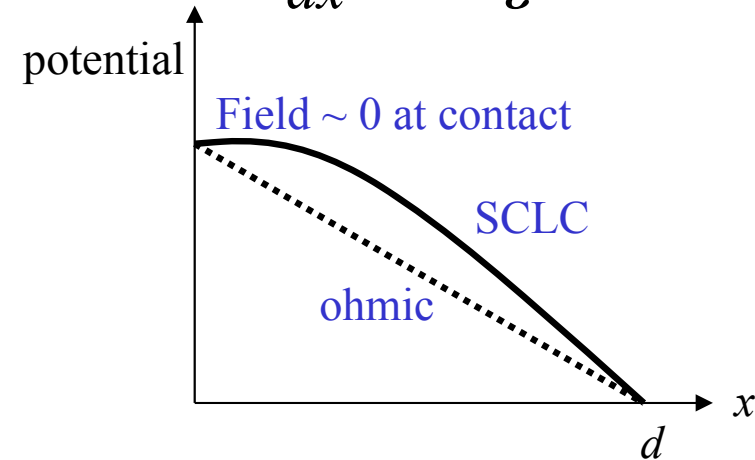
$$= \left(\frac{CV}{d \cdot \text{area}} \right) \times (\mu E)$$

$$= \frac{\epsilon_0 \epsilon_r}{d^2} \cdot V \cdot \mu \cdot \frac{V}{d}$$

$$= \frac{\epsilon_0 \epsilon_r \mu V^2}{d^3}$$

$$J_{SCLC} = \frac{9}{8} \epsilon_0 \epsilon_r \mu \frac{V^2}{d^3}$$

$$\frac{d^2 V}{dx^2} = -\frac{\rho}{\epsilon}$$



SCLC: no trap

Distribution function of trap density

$$h(E,x) = N_t(E)S(x).$$

Poisson equation : $\frac{dF(x)}{dx} = \frac{\rho}{\epsilon} = \frac{q[p(x) + p_t(x)]}{\epsilon}$.

Current flow equation : $J = q\mu_p p(x)F(x)$.

$$p_t(x) = \int_{E_l}^{E_u} h(E,x)f_p(E)dE, \quad p(x) = N_v \exp\left[-\frac{E_{F_p}}{k_B T}\right].$$

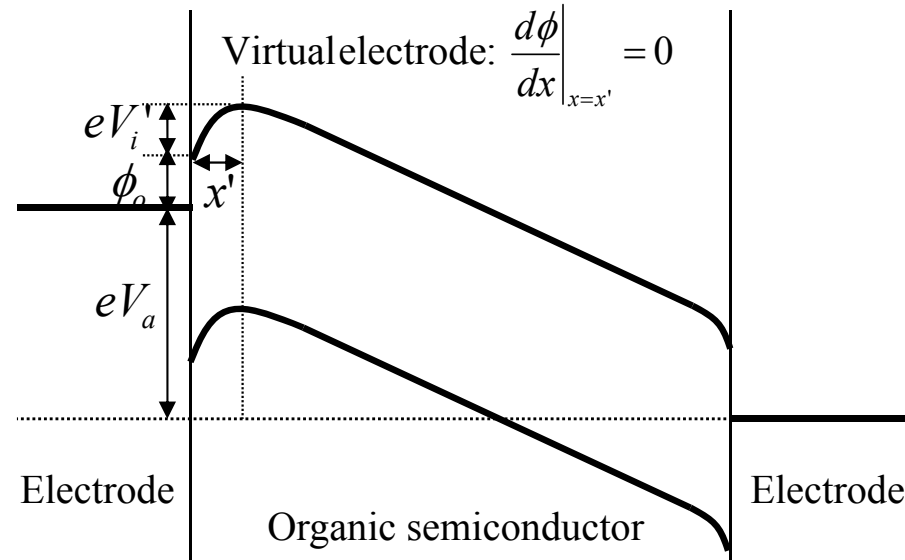
For $p_t(x) = 0$,

$$2F(x)\frac{dF(x)}{dx} = \frac{d[F(x)]^2}{dx} = \frac{2J}{\epsilon\mu_p}. \quad \therefore [F(x)]^2 - [F(x=0)]^2 = [F(x)]^2 = \frac{2J}{\epsilon\mu_p}x.$$

$$\therefore F(x) = \sqrt{\frac{2J}{\epsilon\mu_p}x}.$$

Boundary condition, $V = \int_0^d F(x)dx$.

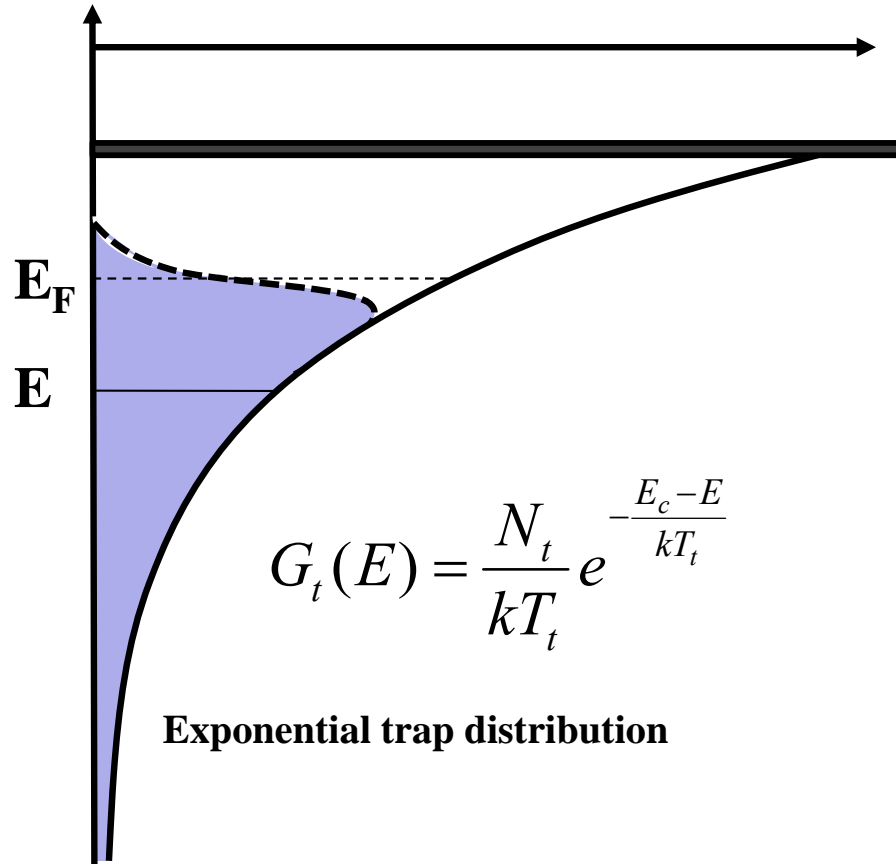
$$J = \frac{9}{8}\epsilon\mu_p \frac{V^2}{d^3}. \quad \text{Mott - Gurney law. (no trap)}$$



The distance W_a between the actual electrode surface and the virtual anode ($-dV/dx = F = 0$) is so small that we can assume $F(x=W_a \rightarrow 0) = 0$ for simplicity.

SCLC: exponential trap density

Energy



$$G_t(E) = \frac{N_t}{kT_t} e^{-\frac{E_c - E}{kT_t}}$$

DOS

E_C (E_{LUMO})

$$n_f = N_c e^{-\frac{E_c - E_F}{kT}}$$

$$n_t = \int_{-\infty}^{E_c} \frac{N_t}{k_B T_t} e^{-\frac{E_c - E}{kT}} f_{FD}(E) dE$$

$$\approx \int_{-\infty}^{E_F} \frac{N_t}{k_B T_t} e^{-\frac{E_c - E}{kT}} dE$$

$$= N_t e^{-\frac{E_c - E_F}{kT_t}}$$

$$\therefore n_t \approx N_t \left(\frac{n_f}{N_c} \right)^{\frac{T}{T_t}} = N_t \left(\frac{n_f}{N_c} \right)^{\frac{1}{m}}$$

$$m = \frac{T_t}{T}$$



SCLC: exponential trap density

$$\text{Poisson equation : } \frac{dF(x)}{dx} = \frac{q[n_f(x) + n_t(x)]}{\epsilon_0 \epsilon} \approx \frac{qn_t(x)}{\epsilon_0 \epsilon} \approx \frac{qN_t}{\epsilon_0 \epsilon} \left(\frac{n_f}{N_c} \right)^{1/m}.$$

$$\text{Current flow equation : } J = q\mu n_f(x)F(x).$$

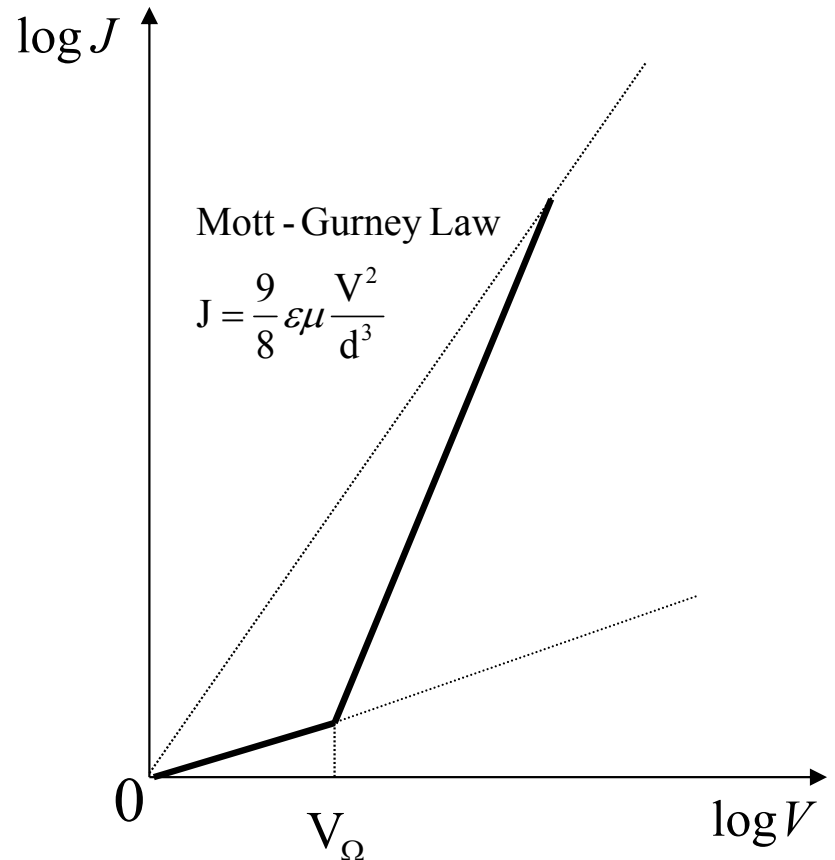
$$F^{1/m} \frac{dF(x)}{dx} = \frac{N_t}{\epsilon_0 \epsilon} \left(\frac{J}{q\mu N_c} \right)^{1/m}.$$

$$\therefore \frac{m}{m+1} F^{\frac{m+1}{m}} = \frac{N_t}{\epsilon_0 \epsilon} \left(\frac{J}{q\mu N_c} \right)^{1/m} x.$$

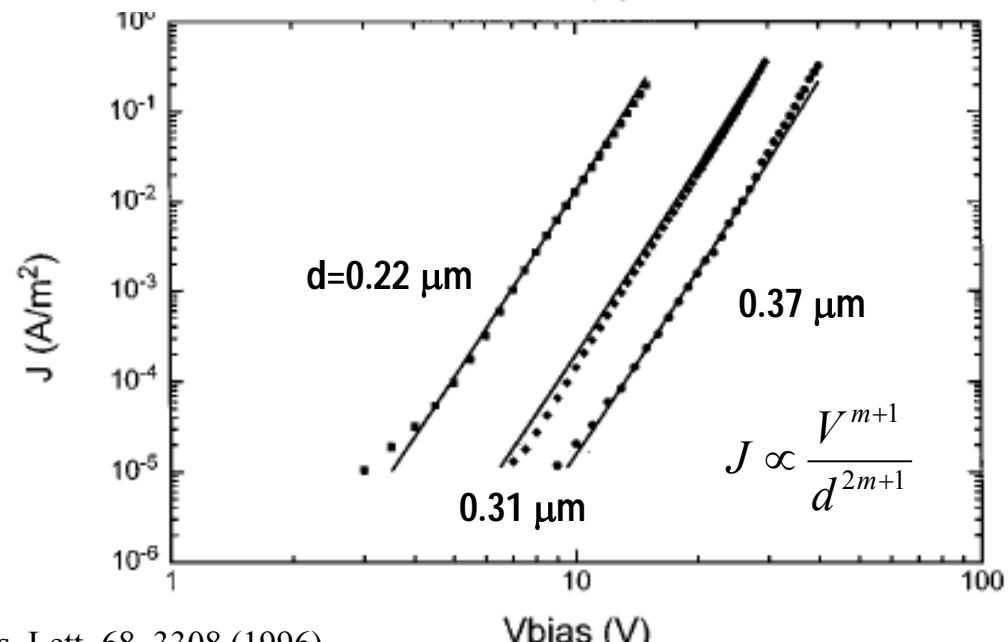
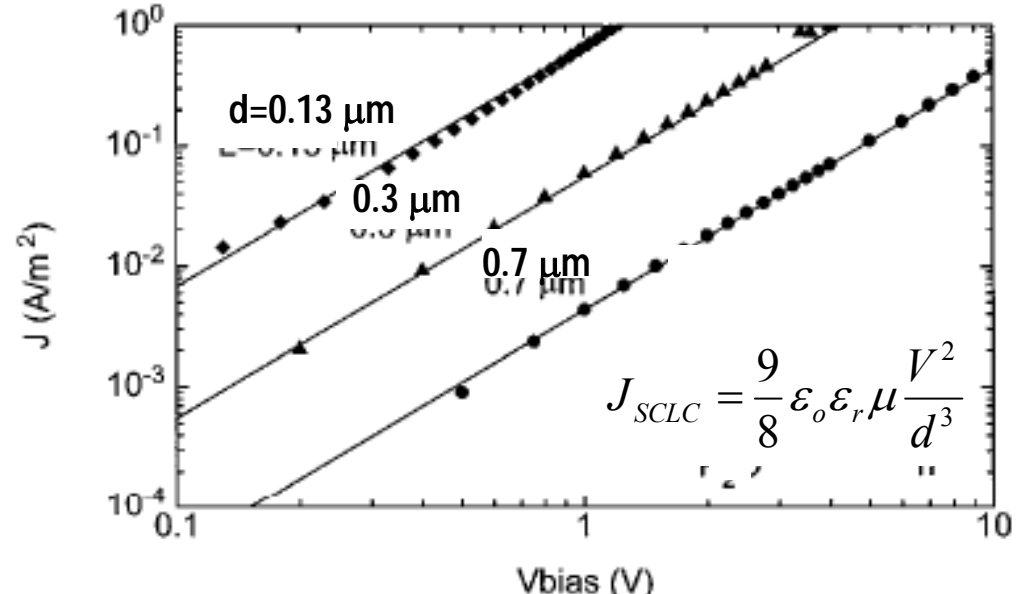
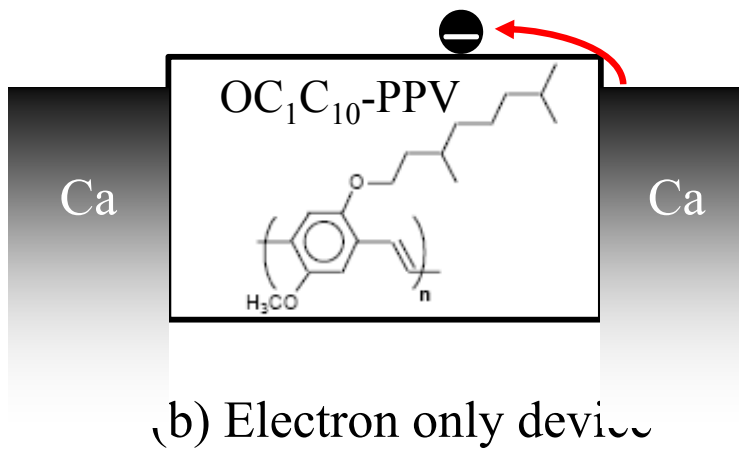
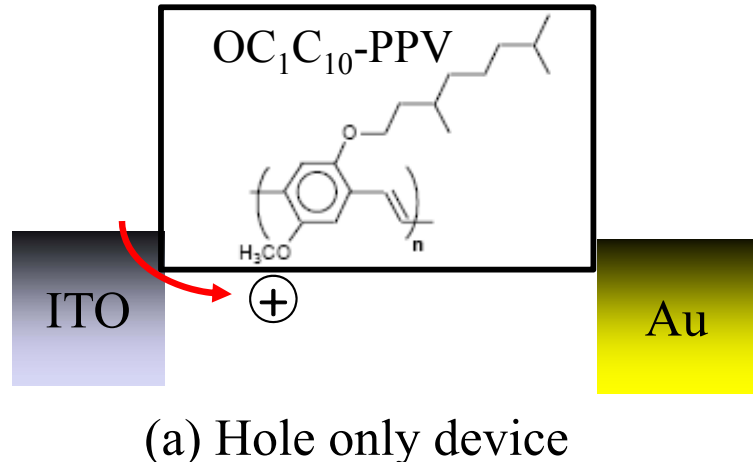
$$\therefore F(x) = \left(\frac{m+1}{m} \frac{N_t}{\epsilon_0 \epsilon} \right)^{\frac{m}{m+1}} \left(\frac{J}{q\mu N_c} \right)^{\frac{1}{m+1}}.$$

$$\text{Boundary condition, } V = \int_0^d F(x) dx.$$

$$J = q^{1-m} \mu N_c \left(\frac{2m+1}{m+1} \right)^{m+1} \left(\frac{m}{m+1} \frac{\epsilon_0 \epsilon}{N_t} \right)^m \frac{V^{m+1}}{d^{2m+1}}, \quad m = \frac{T_t}{T}.$$



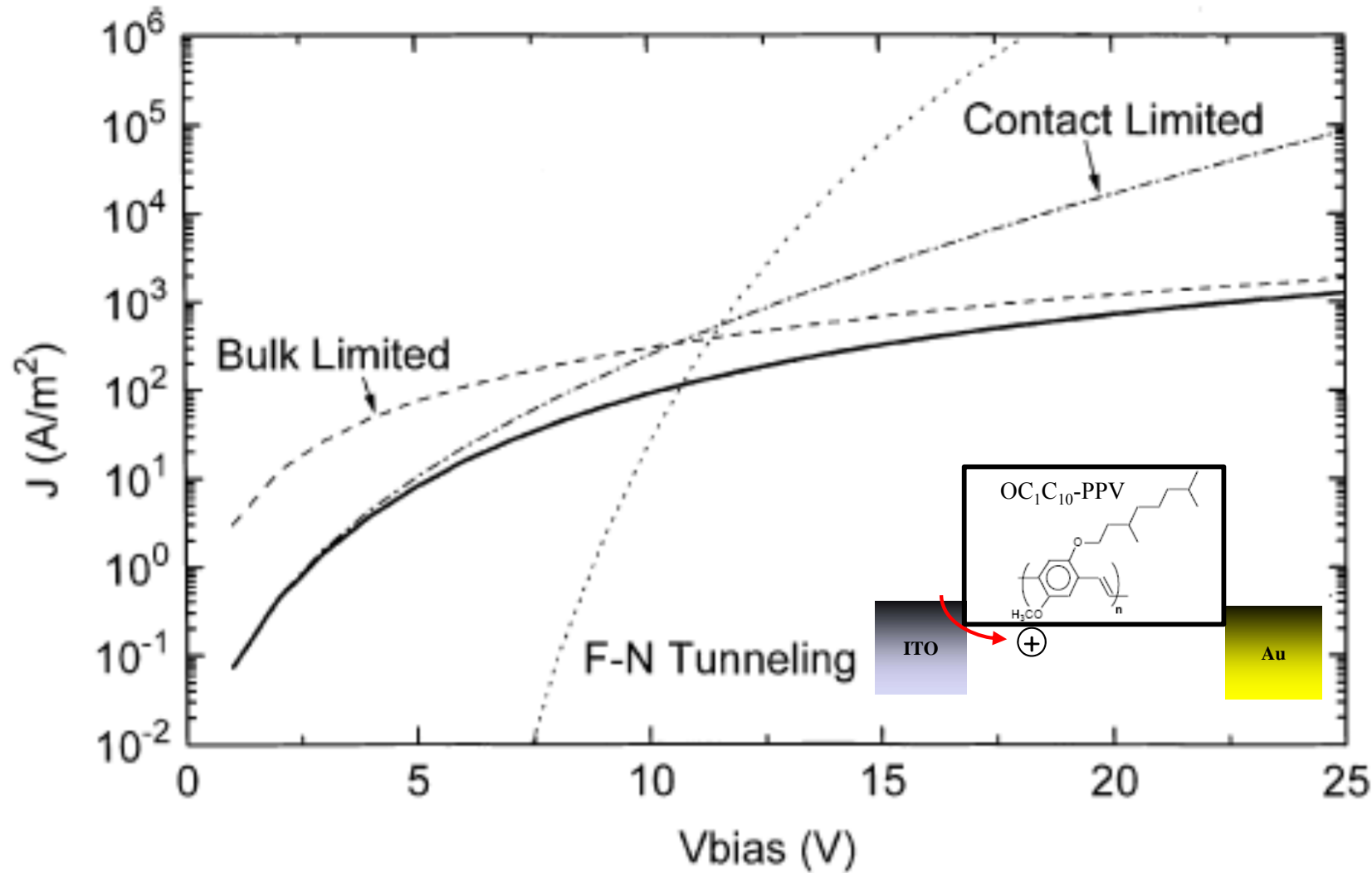
SCLC: an example



P. W. M. Blom M. J. M. de Jong, and J. J. M. Vleggaar, Appl. Phys. Lett. 68, 3308 (1996).



SCLC: comparison with other models



P. W. M. Blom M. J. M. de Jong, and J. J. M. Vleggaar, Appl. Phys. Lett. 68, 3308 (1996).

